Multiscale Mechanobiology of Primary Cilia

An M. Nguyen

Submitted in partial fulfillment of the

requirements for the degree

of Doctor of Philosophy

in the Graduate School of Arts and Sciences

COLUMBIA UNIVERSITY

2015

ABSTRACT

Multiscale Mechanobiology of Primary Cilia

An M. Nguyen

Mechanosensation, the ability for cells to sense and respond to physical cues, is a ubiquitous process among living organisms and its dysfunction can lead to devastating diseases, including atherosclerosis, osteoporosis, and cancer. The primary cilium is a solitary, immotile organelle that projects from the surface of virtually every cell in the human body and can function as a mechanosensor across diverse biological contexts, deflecting in response to fluid flow, pressure, touch, and vibration. It can detect urinary flow rate in the kidney, monitor bile flow in the liver, and distinguish the direction of nodal flow in embryos. In this thesis, we examined the interplay of biology and mechanics in the context of this multifunctional sensory organelle from the tissue to subcellular scale.

In the first part of this work, we examined the cilium at the tissue level. Primary cilia are just beginning to be appreciated in bone with studies recently reporting loss of cilia results in defects in skeletal development and adaptation. We disrupted primary cilia in osteocytes, the principal mechanosensing cells in bone, and demonstrated that loss of primary cilia in osteocytes impairs load-induced bone formation. Over the course of our work with primary cilia, we also identified the need for more standardized imaging approaches to the cilium and presented an improvement to distinguishing proteins within the cilium from the rest of the cell.

In the later part of this work, we examined the primary cilium at the subcellular

level. While deflection is integral to the cilium's mechanosensory function, it remains poorly understood and characterized. Using a novel combination of experimental and computational techniques to capture and determine the mechanical properties of the cilium, we demonstrated cilium deflection can be mechanically and chemically modulated. We revealed a mechanism, acetylation, through which this mechanosensor can adapt and regulate overall cellular mechanosensing. By modifying our combined experimental and computational approach, we analyzed cilium deflection *in vivo* for the first time.

Collectively, this work uncovers new insights across biological scales in the primary cilium as an extracellular nexus integrating mechanical stimuli and cellular signaling. Understanding the mechanisms driving cilium mechanosensing has broad reaching implications and unlocks the cilium's potential as a therapeutic target to treat impaired cellular mechanosensing critical to a multitude of diseases.

Contents

List of Figures

List of Tables

Acknowledgments

This dissertation would not have been possible without the support and collaboration of many and this is an accomplishment that I share with them. The acknowledgements that follow only highlight the contributions made.

I thank my advisor, Dr. Chris Jacobs, for his invaluable guidance, high expectations, tough love approach and his continued patience with my struggles in writing. I have especially appreciated our shared interest in cycling and the many anecdotes that have arisen from it. The community provided by our lab has been a great opportunity for me to explore and learn. I especially Dr. Julia Chen and Dr. David Hoey for their advice, technical support and collaboration. I have also appreciated the many years having Dr. Kristen Lee as a desk and lab partner from sharing ideas and asking questions interspersed with pictures of cute dogs.

Before Chris, there were many other advisors who have contributed to this journey. I thank Chris Brown, Dr. Robert Williams and Dr. Michael Launder for giving me early opportunities to explore research. At Penn, I thank Dr. Steve Nicoll, Dr. Ken Foster, Dr. Max Mintz, Dr. Harriet Joseph, Dr. Sonya Gwak, and Dr. Joe Sun for their mentorship inside and outside of the classroom and support of my research endeavors. I am grateful to my undergraduate advisor, Dr. Dawn Elliott,

and my unofficial advisor, Dr. Rob Mauck, for shaping me as a researcher and their continued advice many years later. At Stanford, I thank Dr. Alesha Castillo, Dr. James Chang, Dr. Ben Barres, and Dr. Sally Gressens for reminding me of my love for the lab and research.

I am grateful to the many colleagues from whom I have learned so much. I am especially grateful to Dr. Wade Johannessen and Dr. Nandan Nerurkar who took the time during their graduate work to teach and mentor me as an undergraduate. I thank Dr. Sounok Sen for setting the bar as a colleague in the lab and friend outside of the lab. Many colleagues at Columbia have also been helpful in research discussions and I have appreciated their friendship: Genevieve Brown, Gwen Effgen, Dr. Venk Hariharan, Dr. Grace O'Connell, Dr. Corina Curschellas, Dr. Keenan Bashour, Dr. Brian Gillette, and Dr. John Finan.

The research presented in this dissertation is a reflection of much collaboration. I thank my proposal and dissertation committee members for their time reviewing and providing feedback and I appreciate their insight and critical evaluation in molding this work. I thank our lab manager, Keith Yeager, for his resourcefulness and creativity in solving the many problems I bring to him. I also thank our department administrators, Shila Maghji, Kidest Shenkoru, Jarmaine Lomax, Michelle Cintron, and Paulette Louissant, and animal facility staff, Dr. Kevin Prestia, Dr. Kelly Yamada, Vivian Carbonell, Haydee Velez, Ed Torres, and Vaughn Francis, for keeping everything running smoothly. Of course, research is not possible without funding and support and several sources have supported this work, including an NSF Graduate Research Fellowship, NIH grants T32 AR059038, R21 AR054156, R01 AR045989, and R01 AR062177.

Finally, on a more personal note, I am grateful to the community around me that have been a source of constant love and support. I cannot thank Sheriza, Chandni, Janny and Luciano enough for being there through it all for a decade and counting. A special thank you goes to Rebecca, Gavi, Macke, Rick for adopting me into their families. I thank my cycling sisters, Angelica, Chrissy, Cristina, Gemma, Ginna, and Valerie, for getting me out of the lab regardless of the weather and showing me there is so much more to NYC. I thank my academically-oriented friends, Chand, Gwen, Genevieve, Corina, Grace, and Kat, who have empathized with me on life as a PhD student. In addition, I appreciate the Dorm Room Fund community who are absolutely inspiring and thank Phin, CeCe, Jahan, David, and Paul who have mentored me as I transition to life after school. Lastly, I thank Shadow and her many friends who have made the hours of analyzing data, reading papers and writing infinitely more enjoyable with their company and occasional shenanigans.

For those who have supported me through this journey

and given new meaning to family

Chapter 1

Introduction

1.1 Mechanosensing

Mechanical signals are critical to many biological processes and the ability for cells to sense and respond to these signals is termed mechanosensing. At the organismal level, mechanosensing helps the cardiovascular system maintain and regulate blood pressure [Tarbell *et al.*, 2014], the skeletal system adapt to its loading environment [Robling *et al.*, 2006], and the auditory system detect sound waves [Schwander *et al.*, 2010]. At the cellular level, mechanosensing can direct motility, differentiation, proliferation, and apoptosis [Janmey and McCulloch, 2007]. At the subcellular and molecular levels, mechanosensors are the structures that sense mechanical signals through force-induced conformational or other physical changes. They can be a small complex of proteins that form focal adhesions to the entire cytoskeleton that detect forces in the extracellular matrix and neighboring cells [Hirata *et al.*, 2014]. Not surprisingly, dysfunction in mechanosensing can lead to devastating diseases, including atherosclerosis, osteoporosis, and cancer [Hoffman *et al.*, 2011].

1.2 Primary cilia mechanosensing

Previously thought to be of little functional importance [Federman and Nichols, 1974], the primary cilium is now recognized as an emerging mechanosensor. The cilium is a single, immotile multifunctional sensory organelle that extends from the cell surface of nearly every mammalian cell. Recently, renewed interest in this organelle has led to numerous studies and insights into the primary cilium's

structure and function. As a mechanosensor, the cilium deflects in response to flow, pressure, touch, and vibration [Singla and Reiter, 2006]. Primary cilia monitor bile and urinary flow in the liver and kidney, respectively [Masyuk *et al.*, 2006; Praetorius and Spring, 2001; Praetorius and Spring, 2003]. In developing nodes, primary cilia detect the direction of nodal flow [McGrath *et al.*, 2003]. Primary cilia have recently been implicated in sensing blood flow in blood vessels [Nauli *et al.*, 2008] and lacunocanalicular flow in bone and cartilage [Malone *et al.*, 2007; McGlashan *et al.*, 2010; Xiao *et al.*, 2006].

1.3 Ciliopathies

Disorders involving defects in cilia structure and function are now known as ciliopathies. Not surprisingly, these defects often result in multisystemic dysfunction due to the cilium found on virtually every cell in the body. Renal disease, retinal degeneration and cerebral anomalies are common features of ciliopathies [Waters and Beales, 2011]. Primary cilia have been the most studied in the context of kidney. In 2000, Murcia et al. observed that a mutation in the *Tg737* gene resulted in left-right asymmetry in mice [Murcia *et al.*, 2000]. The same mutation also led to defects in the cilium. In addition to Ift88, the protein encoded by *Tg737*, Kif3a, Polycystin 1, and Polycystin 2, among other ciliary proteins, has been associated with ciliopathies [Lin *et al.*, 2003; Yoder, 2002].

1.4 Primary cilia biology

The cilium is a microtubule-based structure, where the axoneme consists of nine microtubule doublets that extend from the basal body (Fig. 1.1). These doublets provide the cilium its structural integrity. In contrast to other cellular projections, the motile cilium and flagellum, the primary cilium lacks two central microtubules and other axonemal components, including radial spokes, Dynein arms and Nexin links [Schwartz *et al.*, 1997], that are thought to reinforce the axoneme. Motile cilia with these components are one order of magnitude stiffer than primary cilia.

Intraflagellar transport (IFT) is the process through which the cilium is formed and maintained. IFT transports proteins along the axoneme to and from the cell. Since the cilium lacks the translation machinery to form proteins, proteins found in the cilium are formed outside of the cilium and IFT transports these proteins to the cilium. Motor proteins are critical in driving this transport system. Kinesin 2 transports proteins away from the cell body towards the cilium tip while Dynein transports proteins in the reverse direction. Two proteins implicated in ciliopathies in an earlier paragraph, Kif3a and Ift88, are also important in IFT. Kinesin 2 consists of two subunits, Kif3a and Kif3b, [Praetorius and Spring, 2005]. Ift88 forms part of the protein complex used to transport and carry other proteins along the axoneme [Kobayashi and Dynlacht, 2011; Lucker *et al.*, 2010].

While primary cilia are found on nearly every cell, the presence of cilia on these cells depends on the cell cycle. The cilium is assembled and resorbed as a cell progresses through the cycle. The cilium is assembled during interphase. The basal

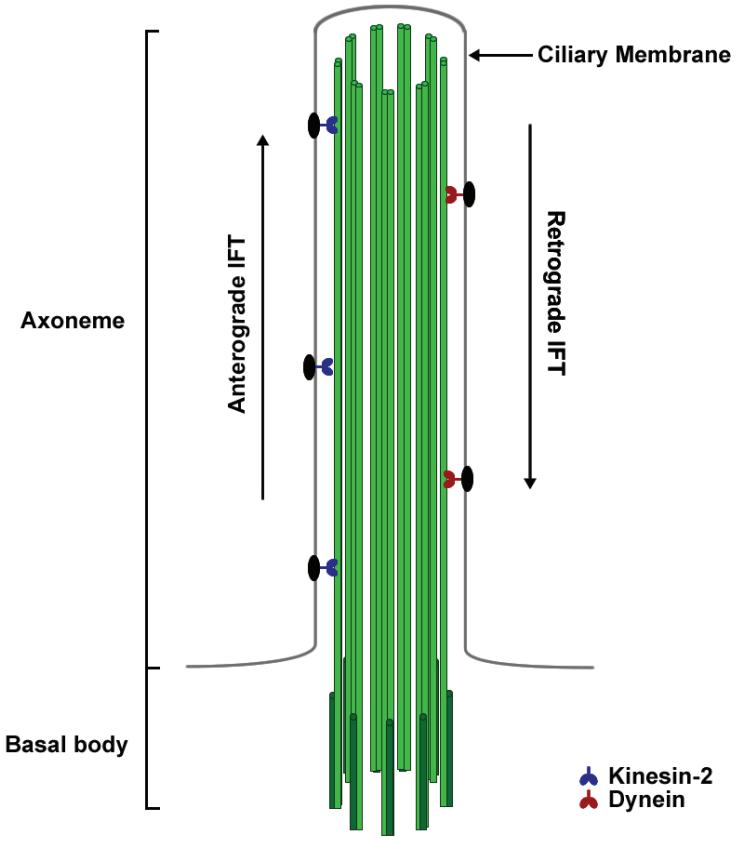

Figure 1.1: Microtubule-based structure of primary cilium. The cilium consists of the axoneme and basal body. Anterograde IFT is driven by Kinesin 2 motors (blue) while retrograde IFT is driven by Dynein motors (red) along the axoneme microtubules (green). Reprinted with permission from [Nguyen and Jacobs, 2013].

body nucleates from the mother centriole and anchors the cilium while the axoneme is formed through IFT by Kinesin 2. The cilium is resorbed before mitosis and entry of the cell cycle. The incidence of cilia is highest on cells arrested in G0-G1 [Quarmby and Parker, 2005; Wheatley *et al.*, 1996].

1.5 Modeling primary cilia mechanics

Primary cilia bending was first modeled by Schwartz et al. where the cilium was modeled as an elastic beam using the small-rotation Euler-Bernoulli formulation [Schwartz *et al.*, 1997]. The authors estimated cilium stiffness of rat kangaroo kidney cells to be on the order of 10^{-23} Nm^2. Building on this model, Liu et al. added a more accurate description of flow-induced loading using Stokes equations [Liu *et al.*, 2007] and Downs et al. used a large rotation formulation [Downs *et al.*, 2012]. With a more sophisticated approach that accounted for rotation at the base of the cilium and the cilium's initial configuration, the authors reported stiffness for mouse kidney cells on the order of 10^{-22} Nm^2, which is an order of magnitude higher than reported by Schwartz et al. [Schwartz *et al.*, 1997]. Advances in bending analysis of cilia have suggested that the cilium is a dynamic organelle, capable of structural changes in response to its environment. Recently, Besschetnova et al. demonstrated cilia length is modulated by flow [Besschetnova *et al.*, 2010] and Rich and Clark demonstrated cilia length is modulated by osmolarity [Rich and Clark, 2012].

1.6 Motivation

Although physical cues are vitally involved in a breadth of physiological processes, mechanosensing is complex and remains poorly understood. The primary cilium has recently emerged as a nexus capable of integrating physical signals and coordinating biochemical responses across biological scales. At the tissue level, bone, constantly responding and adapting to physical loads, is an exciting context to study primary cilium mechanosensing. While primary cilia have been implicated in bone adaptation and formation, it is not known if osteocytes, the principal mechanosensing cells in bone, use primary cilia *in vivo* to detect physical loads [Tatsumi *et al.*, 2007]. At the subcellular level, the kidney cilium is the ideal system to study mechanosensing. Specifically the long kidney cilium's deflection in response to fluid flow is easily visualized with fluorescence microscopy [Downs *et al.*, 2012; Mitchell *et al.*, 2009; Young *et al.*, 2012]. In this context, recent data have suggested the cilium's capacity to adapt as a mechanosensor. A greater understanding of the cilium as an extracellular nexus adapting to and integrating mechanical stimuli and cellular signaling not only contributes to the primary cilia field but also the broader field of mechanosensing. With cellular mechanosensing critical to a multitude of diseases and the primary cilium such a ubiquitous mechanosensor, the cilium is a therapeutic target of high value.

1.7 Organization

This dissertation contains four investigations advancing the understanding of primary cilium mechanosensing across biological scales. In chapter 2, we use a conditional knockout mouse model to demonstrate the osteocyte primary cilium's role in sensing load and coordinating the bone formation response. In chapter 3, we describe the challenges with identifying proteins in the cilium and develop a method to distinguish ciliary and cytosolic pools of proteins. In chapter 4, we use combined experimental and computational methods to show the primary cilium adapts to stimuli through a mechanism involving acetylation. In chapter 5, we apply our computational method to characterize primary cilia deflection *in vivo*. This dissertation concludes with chapter 6 discussing contributions, limitations and future areas of research motivated by the works discussed in chapters 2-5.

Chapter 2

Primary cilia mechanosensation in bone by osteocytes *in vivo*

Collaborators on this project are Marie D. Guevarra, Samuel T. Robinson, X. Edward Guo, and Christopher R. Jacobs.

2.1 Abstract

Previous studies have demonstrated the primary cilium plays a role in sensing physical loads in bone. Because findings from these studies were confounded, the osteocyte primary cilium's role *in vivo* remains unclear. Prior studies deleted *Kif3a* and though it is a motor protein used in intraflagellar transport, *Kif3a* also has a non-ciliary role. In addition, *Kif3a* was deleted in both osteoblasts and osteocytes. The goal of this study was to specifically determine the osteocyte primary cilium's mechanosensory role. We addressed this by targeting *Ift88*, a cilia-specific protein also involved in intraflagellar transport. Using *Dmp1-Cre* and *Ift88* floxed mice, we developed conditional knockout mice with primary cilia-deficient osteocytes. We found that this targeted deletion of *Ift88* did not affect skeletal development but did inhibit cilia formation. We then loaded ulnae of 16-week-old mice and measured 47% reduction in loading-induced bone formation in the conditional knockout mice. These data provide the first specific *in vivo* demonstration of the osteocyte primary cilium's role in bone mechanosensation.

2.2 Introduction

As studies have continued to identify new contexts in which primary cilia play a mechanosensory role, the cilium has emerged as an important mechanosensor in bone. The concept of the osteocyte primary cilium sensing strain in bone was first proposed about a decade ago [Whitfield, 2003]. In the past decade, groups have now identified cilia in bone [Malone *et al.*, 2007; Xiao *et al.*, 2006] and demonstrated *in vitro* that cilia are involved in bone mechanotransduction. A study by Malone et al. showed that flow-induced osteogenic gene expression is reduced with loss of cilia by siRNA knockdown or chloral hydrate [Malone *et al.*, 2007]. In other studies, loss of cilia by chloral hydrate led to inhibition of flow-induced mineral deposition [Delaine-Smith *et al.*, 2014] and loss of cilia by siRNA knockdown inhibited flow-induced cyclic AMP signaling [Kwon *et al.*, 2010]. Recently, studies have identified the polycystin complex in bone primary cilia [Qiu *et al.*, 2012b; Xiao *et al.*, 2006]. This complex is made up of Polycystin 1 and 2 and have previously been implicated in other cilia-mediated mechanosensing contexts, including kidney and liver. When *Pkd1*, the gene encoding Polycystin 1, is disrupted in osteoblasts, osteogenic gene expression and flow-induced cyclic AMP signaling are attenuated [Qiu *et al.*, 2012b]. Hoey et al. recently suggested that osteocyte cilia are involved in paracrine signaling that induces osteogensis of mesenchymal stem cells [Hoey *et al.*, 2011]. When osteocyte cilia are disrupted by knockdown of *Ift88*, the authors showed the osteogenic response in mesenchymal stem cells was lost.

While primary cilia in bone have predominantly been studied *in vitro*, two recent studies have provided *in vivo* evidence of the cilium's role in osteogenesis.

Both studies targeted *Kif3a*, which encodes a subunit of Kinesin 2 and is important in anterograde intraflagellar transport. Conditional knockouts, however, must be generated because global knockouts of *Kif3a* are embryonically lethal [Marszalek *et al.*, 1999; Qiu *et al.*, 2012a; Temiyasathit *et al.*, 2012]. Temiyasathit et al. deleted *Kif3a* in early osteoblasts through osteocytes using a 2.3 kb fragment of *α1(I)-collagen* promoter to drive *Cre* expression [Dacquin *et al.*, 2002; Liu *et al.*, 2004; Temiyasathit *et al.*, 2012]. This conditional knockout of *Kif3a* resulted in normal skeletal morphology in mice but attenuated the bone formation response to loading. Qiu et al. deleted *Kif3a* in more mature osteoblasts through osteocytes using a 3.9 kb fragment of the osteocalcin promoter [Jiang *et al.*, 2004; Qiu *et al.*, 2012a]. In contrast to the focus on the bone formation response by Temiysathit et al., these authors focused on *Kif3a*'s role in skeletal development and demonstrated that conditional knockout of *Kif3a* led to an osteopenic phenotype in 6-week-old mice, including reduced bone mineral density, bone volume fraction and cortical thickness. The osteopenic phenotype observed at the tissue level was supported by reduced osteogenic gene expression in cells from 6-week-old mice. By 24 weeks, skeletal development recovered and mice no longer had a measureable osteopenic phenotype. While these data implicate cilia in skeletal development and formation, these data do not distinguish the role of osteoblast from osteocyte cilia in these processes.

The key mechanosensing cell in bone is the osteocyte and in adult bone, osteocytes are the predominant cell type [Bonewald, 2011]. By showing that ablating osteocytes protected mice from unloading-induced bone loss, Tatsumi et al. established the osteocytes role in bone mechanotransduction [Tatsumi *et al.*, 2007]. We expand on these findings and hypothesize that the osteocyte can sense physical loads through the primary cilium. Although previous studies have suggested

the osteocyte primary cilium is involved in bone mechanosensing, no study has demonstrated this *in vivo*. Findings of previous studies did not distinguish the role of primary cilia in osteoblasts and osteoblasts and targeted a gene with a role both inside and outside the cilium [Qiu *et al.*, 2012a; Temiyasathit *et al.*, 2012]. Because the promoters used in previous studies resulted in Cre recombination in osteoblasts and osteoblasts mature into osteocytes, loss of *Kif3a* also occurs in the terminally differentiated osteocytes. Consequently the contributions of cilia in the previous studies cannot be discriminated between the osteoblast and osteocyte population. Additionally, although *Kif3a* is involved in anterograde IFT, *Kif3a* is also involved in Wnt signaling [Corbit *et al.*, 2008]. When *Kif3a* is disrupted, Dishevelled is constitutively phosphorylated and β-catenin accumulates in the cytoplasm. This suggests that in addition to its ciliary role, *Kif3a* can regulate the Wnt/β-catenin pathway that is important in skeletal development [Day *et al.*, 2005; Galli *et al.*, 2010; Holmen *et al.*, 2005; Kramer *et al.*, 2010; Tu *et al.*, 2012]. The osteopenic observations in 6-week-old mice discussed in the previous paragraph may be attributed to *Kif3a*'s non-ciliary role [Qiu *et al.*, 2012a]. By using *Dmp1 (Dentin matrix protein1)-Cre* and *Ift88* mice to develop a conditional knockout of cilia in osteocytes, we can address both issues. *Dmp1* is specifically expressed in osteocytes [Yang *et al.*, 2005] and *Ift88* has a specific ciliary role [Corbit *et al.*, 2008].

Using these mice with an osteocyte-specific deletion of primary cilia, we examined the osteocyte cilium in loading-induced bone formation. *In vivo* ulnar loading is one method in which to study skeletal adaption. With this loading model, our lab has shown the role of β1 integrins, Kif3a, and adenylyl cyclase 6 in mechanical adaption of bone [Lee *et al.*, 2014; Litzenberger *et al.*, 2009; Temiyasathit *et al.*, 2012]. A recent study using *Dmp1-Cre* to delete *Pkd1* in

osteocytes showed that mice were osteopenic in addition to impaired loading-induced bone formation [Xiao *et al.*, 2011].

The purpose of this study was to distinguish the osteocyte primary cilium's mechanosensory role in skeletal adaptation that had been implicated by previous studies. Conditional deletion of cilia-specific gene *Ift88* resulted in loss of osteocyte cilia. Because skeletal morphology was not affected by the loss, our data suggest that osteocyte cilia do not play a role in skeletal development. Our data also show loss of osteocyte cilia in mice led to impaired skeletal adaptation. Collectively, these data directly demonstrate the osteocyte primary cilium plays a role in skeletal adaptation and suggest this organelle may be targeted in treatments for bone loss.

2.3 Methods

2.3.1 Animals

Dmp1-Cre mice were obtained from Lynda Bonewald at the University of Missouri-Kansas City [Lu *et al.*, 2007]. *Ift88*$^{fl/fl}$ and *Ift88*$^{fl/null}$ mice were obtained from Bradley Yoder at the University of Alabama at Birmingham [O'Connor *et al.*, 2013]. Using male *Dmp1-Cre* and female *Ift88*$^{fl/null}$ mice, male *Dmp1-Cre;Ift88*$^{+/null}$ mice were generated and then crossed with female *Ift88*$^{fl/fl}$ mice. The *Dmp1-Cre;Ift88*$^{fl/null}$ and *Ift88*$^{fl/+}$ offspring used in the experiments. To avoid any potential Cre activity through the female germline, the *Cre* transgene was transmitted specifically through the male [Liang *et al.*, 2009; O'Connor *et al.*, 2009]. Genomic DNA was obtained from tail biopsies and used in PCR analysis to genotype mice (Table 1). For the *Cre* PCR reaction, *myogenin* was used as a positive control. Male *Dmp1-Cre* mice and female *Rosa26R* reporter mice were used to generate *Dmp1-Cre;Rosa26R* mice and assess *Cre* recombination [Lu *et al.*, 2007]. The procedures performed in this study were in accordance with Columbia University Institutional Animal Care and Use Committee guidelines.

Primer	**5' to 3' Sequence**
Ift88 common forward	GCCTC CTGTT TCTTG ACAAC AGTG
Ift88 floxed & wildtype reverse	GGTCC TAACA AGTAA GCCCA GTGTT
Ift88 null reverse	CTGCA CCAGC CATTT CCTCT AAGTC ATGTA
Cre forward	GAACC TGATG GACAT GTTCA GG
Cre reverse	AGTGC GTTCG AACGC TAGAG CCTGT
Myogenin forward	TTACG TCCAT CGTGG ACAGC
Myogenin reverse	TGGGC TGGGT GTTAG CCTTA

Table 2.1: Custom primers used in PCR-based genotyping. *Ift88* primers were used in one set of reactions while Cre and Myogenin primers were used in a separate set of reactions.

2.3.2 *In vivo* axial ulnar loading

At 16 weeks, *Dmp1-Cre;Ift88*$^{+/null}$ and *Ift88*$^{fl/+}$ mice were loaded as previously described [Lee *et al.*, 2014; Litzenberger *et al.*, 2009; Temiyasathit *et al.*, 2012]. Briefly, with mice under isoflurane-induced anesthesia, right forelimbs were loaded axially at 120 cycles per day for 3 consecutive days with a 2Hz sine waveform and 3N peak load using an EnduraTEC-ELF 3200 electromechanical loading system (Bose, Eden Prairie, MN). The non-loaded left forelimbs were used as internal controls. Between the loading sessions, normal cage activity was allowed. Fluorochrome labeling was administered through subcutaneous injections 5 days and 9 days after the first day of loading, calcein (30 mg/kg body weight; Sigma) and Alizarin Red S (75 mg/kg body weight; Sigma), respectively. At 12 days after the first day of loading, mice were euthanized and ulnae were dissected then fixed in 70% ethanol for processing. Tibiae were also dissected and stored at -20°C until further analysis.

2.3.3 Dynamic histomorphometry

Ulnae were embedded in methyl methacrylate as previously described [Lee *et al.*, 2014; Litzenberger *et al.*, 2009; Temiyasathit *et al.*, 2012]. Using an IsoMet 1000 diamond saw (Buehler, Lake Bluff, IL), ulnae were sectioned at the midshaft and sections were imaged on a confocal microscope (TCS SP5; Leica, Wetzlar, Germany) with a 20× objective (0.7 NA). Histomorphometric parameters were measured: bone perimeter (B.Pm), single labeled perimeter (sL.Pm), double labeled perimeter (dL.Pm), and double label area (dL.Ar). Standard measures of bone formation were also determined at the periosteal surface using custom Matlab code

[Dempster *et al.*, 2013]: mineral apposition rate [**MAR** (μm/day) = $\frac{dl.AR/dl.Pm}{4 \text{ days}}$], mineralizing surface [**MS/BS**(%) = $\frac{0.5 \times sL.Pm + dL.Pm}{B.Pm} \times 100$] and bone formation rate [**BFR**($\mu m^3/\mu m^2$/year) = **MAR** × **MS/BS** × 365 days]. Within individual animals, non-loaded values were subtracted from loaded values to calculate relative (r) measurements, indicating increases due to mechanical loading.

2.3.4 Micro-computed tomography (μCT) analysis

Using μCT (Scanco vivaCT 40; Scanco Medical AG, Bruuttisellen, Switzerland), tibiae bone architecture was assessed at 10.5 μm isotropic resolution as previously described [Lee *et al.*, 2014; Litzenberger *et al.*, 2009; Sabsovich *et al.*, 2008; Temiyasathit *et al.*, 2012]. To analyze cortical bone, total area, cortical area, cortical thickness, and minimum and maximum second moments of inertia (I_{min} and I_{max}) was determined at the midshaft. To analyze trabecular bone, bone volume fraction (BV/TV), connective density (Conn. D.), trabecular number (Tb. N.), trabecular thickness (Tb. Th.), and trabecular separation (Tb. Sp.) were determined at the proximal metaphysis [Bouxsein *et al.*, 2010].

2.3.5 Histochemical detection of β-galactosidase activity

At 16 weeks of age, *Dmp1-Cre;Rosa26R* mice were euthanized and ulnae were dissected. After removing epiphyses, ulnae were fixed in 0.25% gluteraldehyde for 5 days at 4°C, decalcified in buffered 0.1M EDTA for 5 days, stained for β-Gal activity overnight at 37°C (1 mg/ml X-gal, 5 mM potassium ferricyanide, 5 mM potassium ferrocyanide, and 1 mM $MgCl_2$), and cryoprotected in 30% sucrose overnight at 4°C

[Cho *et al.*, 2010]. Once ulnae were fixed and stained, they were cryosectioned at 10 μm thickness and imaged on an inverted microscope (CKX41; Olympus, Center Valley, PA) with a 4× objective (0.13 NA).

2.3.6 *In situ* imaging of primary cilia

Epiphyses were removed from previously dissected tibiae of *Ift88*$^{fl/+}$ and *Dmp1-Cre;Ift88*$^{+/null}$ mice. Samples were then fixed in 10% formalin overnight at 4°C, decalcified in RDO Rapid Decalcifier, and cryoprotected in 30% sucrose overnight at 4oC. Samples were cryosectioned at 15 μm in thickness. Sections were permeabilized for 1 hour in 2% Triton-X and blocked in 10% goat serum for 1 hour. Sections were then incubated in a primary antibody solution (anti-acetylated α tubulin, C3B9; Sigma, St. Louis, MO) overnight at 4°C, followed by a secondary antibody solution for 1 hour at room temperature (anti-mouse Alexa 488; Life Technologies, Grand Island, NY), and counterstained with DAPI. A common ciliary marker, acetylated α-tubulin, was used to visualize primary cilia in the sections by confocal microscopy (100× objective, 1.46NA, oil immersion, Leica TCS SP5) [Poole *et al.*, 2001].

2.3.7 Primary bone cell isolation

Serial digestion of calvariae from neonatal mouse pups (age 8-10 days) was used to isolate primary bone cells [Lee *et al.*, 2014]. Briefly, calvariae were dissected and incubated in 2 mg/mL collagenase type II (Worthington) at 37°C on an orbital shaker for 20 minute periods. Cells from the first two periods were discarded. The subsequent four periods (3-6) were pooled to form the primary osteoblast mixture and the three

following periods (7-9) were pooled to form the primary osteocyte mixture.

2.3.8 mRNA expression

The isolated primary cells were cultured in growth media with 10% sera. Once cells were 80% confluent, cells were cultured for 2 days in reduced sera, 1%, to promote cilia formation. Using the Autogen RNA Extraction kit and the Quickgene Mini80 (Autogen; Holliston, MA), RNA was extracted from cell lysate. Then using TaqMan reverse transcription kit (Life Technologies, Grand Island, NY), cDNA was synthesized and analyzed in triplicate by relative quantitative real-time RT-PCR. Relative quantification of the mRNA expression levels was determined using the standard curve method with the following primer-probe pairs: *Ift88* (Mm01313467_m1), *Dmp1* (Mm01208363_m1), and *GAPDH* (4352339E) (Life Technologies, Grand Island, NY). Expression was normalized by housekeeping gene *GAPDH*.

2.3.9 Statistical analysis

Data are presented as mean ± standard error of the mean (SEM). To assess effects of gender and genotype, a 2-way ANOVA was use with a Bonferonni post hoc test to adjust for multiple comparisons. Statistical significance was considered at $p<0.05$.

2.4 Results

Mice with primary cilia-deficient osteocytes were first generated and identified by genotyping (Figure 2.1). *Dmp1-Cre;Ift88*$^{fl/null}$ conditional knockout mice appeared normal at birth and through development with no significant difference in body weight between *Dmp1-Cre;Ift88*$^{fl/null}$ and *Ift88*$^{fl/+}$ mice at time of loading (Table 2.2, $p<0.05$). Analysis of bone architecture also showed no differences between *Dmp1-Cre;Ift88*$^{fl/null}$ and *Ift88*$^{fl/+}$ mice (Table 2.3, $p<0.05$). Since we did not detect differences in skeletal morphology between *Ift88*$^{fl/+}$ and *Dmp1-Cre;Ift88*$^{fl/null}$, we used *Ift88*$^{fl/+}$ as our control.

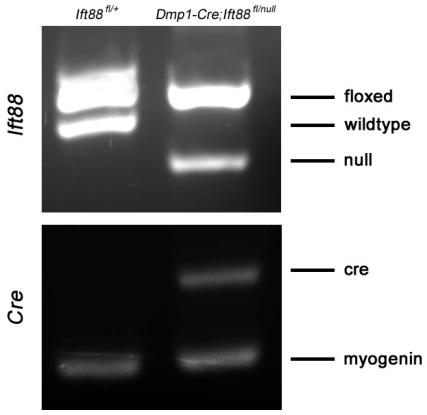

Figure 2.1: Generating an osteocyte-specific deletion of *Ift88* in mice. A typical agarose gel of PCR-based genotyping of DNA from tail biopsies with the following bands: floxed *Ift88* at 370 bp, wildtype *Ift88* at 350 bp, null *Ift88* at 270 bp, *Cre* recombinase at 320 bp and *myogenin* at 250 bp for a positive control in the *Cre* PCR reactions.

Genotype	Males	Females
Ift88$^{fl/+}$	29.0 ± 1.8	22.0 ± 0.5 *
Dmp1-Cre;Ift88$^{fl/null}$	28.6 ± 1.6	22.2 ± 0.4 *

Table 2.2: Body weights of mice measured at 16 weeks. Data presented as mean ± SEM. n = 5 (males), n = 9 (females) for *Ift88*$^{fl/+}$ groups and n = 7 (males), n = 8 (females) for *Dmp1-Cre;Ift88*$^{fl/null}$. * $p < 0.05$ between genders within genotype.

	Males		Females	
	Ift88$^{fl/+}$	*Dmp1-Cre;Ift88*$^{fl/null}$	*Ift88*$^{fl/+}$	*Dmp1-Cre;Ift88*$^{fl/null}$
Parameters				
Cortical, tibia midshaft				
Total area (mm^2)	0.493 ± 0.025	0.505 ± 0.015	0.377 ±0.011	0.378 ± 0.015
Cortical area (mm^2)	0.358 ± 0.016	0.355 ± 0.007	0.276 ± 0.007	0.272 ± 0.007
Cortical thickness (mm^2)	0.189 ± 0.005	0.182 ± 0.001	0.167 ± 0.002	0.164 ± 0.003
I_{max} (mm^4)	0.039 ± 0.005	0.038 ± 0.003	0.020 ± 0.002	0.022 ± 0.001
I_{min} (mm^4)	0.009 ± 0.001	0.009 ± 0.001	0.006 ± 0.001	0.005 ± 0.001
Trabecular, proximal tibia				
BV/TV (%)	21.6 ± 2.0	17.1 ± 1.1	14.6 ± 0.9	13.7 ± 1.0
Tb. N. (mm^{-1})	5.92 ± 0.28	5.25 ± 0.18	4.43 ± 0.10	4.29 ± 0.12
Tb. Th. (mm)	0.051 ± 0.004	0.050 ± 0.003	0.056 ± 0.002	0.054 ± 0.002
Tb. Sp. (mm)	0.167 ± 0.011	0.191 ± 0.017	0.234 ± 0.005	0.244 ± 0.006
Conn. D. (mm^{-3})	219 ± 20	179 ± 16	139 ± 9	150 ± 14

Table 2.3: Bone architecture of mice at 16 weeks. Data presented as mean ± SEM. n = 5 per gender per genotype. * $p < 0.05$ vs. gender-matched controls.

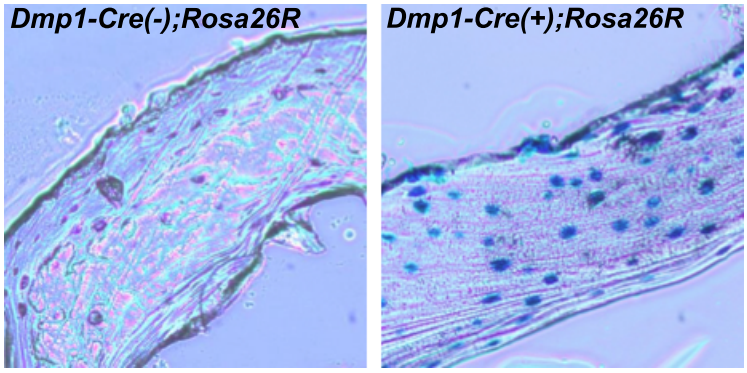

Figure 2.2: Confirming Cre recombination. Cre recombination was detected by X-gal staining (blue). Staining was observed in mice with Cre (right) but was not in mice without Cre (left).

Next, we evaluated effectiveness of *Cre* recombination. To assess its activity, offspring of the heterozygous *Dmp1-Cre* and homozygous *Rosa26R* were stained for β-Gal activity. Staining was detected in *Dmp1-Cre;Rosa26R* mice but not in *Rosa26R* mice without *Dmp1-Cre* (Figure 2.2). To assess the specificity of *Cre* recombination, we isolated primary bone cells and measured gene expression levels of *Dmp1* and *Ift88*. High *Dmp1* expression is characteristic of osteocytes and was observed in the late fractions of cells, indicating the population was predominantly primary osteocytes. Compared to the osteoblasts isolated from the conditional knockout mouse, *Ift88* expression in the isolated osteocytes was reduced by 75%. Although not a complete, *Cre* recombination in osteocytes of the conditional knockout mouse was robust (Figure 2.3). Staining for ciliary marker acetylated α-tubulin in tibiae showed numerous ciliated osteocytes in $Ift88^{fl/+}$ mice compared to few ciliated osteocytes in *Dmp1-Cre;*$Ift88^{fl/null}$ mice, suggesting a loss of cilia with deletion of *Ift88* (Figure 2.4).

Right forelimbs of conditional knockout and control mice were loaded for three consecutive days. Increases in bone formation response, rMS/BS, rMAR, and rBRF/BS, in both conditional knockout and control mice were measured, demonstrating that load induced bone formation in all mice. However, the bone

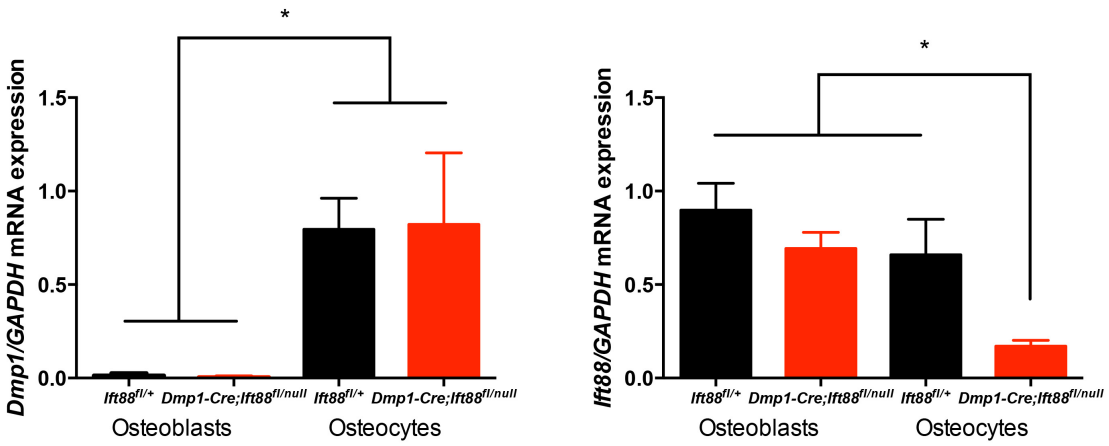

Figure 2.3: *Dmp1* (left) and *Ift88* (right) expression levels in primary cells were normalized to housekeeping gene *GAPDH*. High expression of Dmp1 in primary osteocytes, confirmed osteocytes were predominant in the later fractions. Significant decrease in *Ift88* expression in primary osteocytes from *Dmp1-Cre;Ift88*$^{fl/null}$ mice indicated *Ift88* deletion occurred specifically in osteocytes. Data presented as mean ± SEM. n=7 (osteoblasts), n=3 (osteocytes) for *Dmp1-Cre;Ift88*$^{fl/null}$ and n=6 (osteoblasts), n=3 (osteocytes) for *Ift88*$^{fl/+}$ groups. * $p<0.05$.

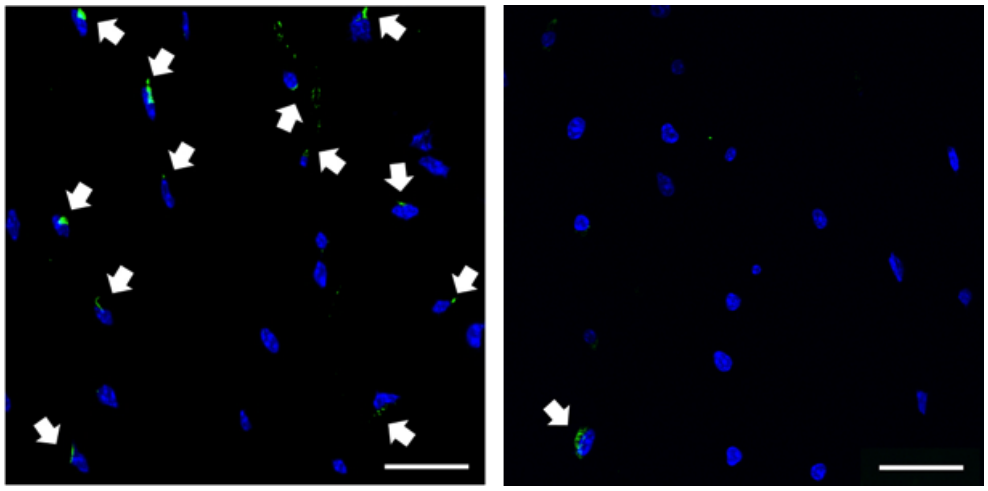

Figure 2.4: Effect of *Ift88* deletion. Ulnae of *Dmp1-Cre; Ift88*$^{fl/null}$ mice (right) showed fewer primary cilia (white arrows) when compared to ulnae of *Ift88*$^{fl/+}$ mice (left). Nuclei are stained with DAPI (blue) and ciliary marker acetylated-α tubulin with C3B9 (green). Scale bar indicates 20 μm.

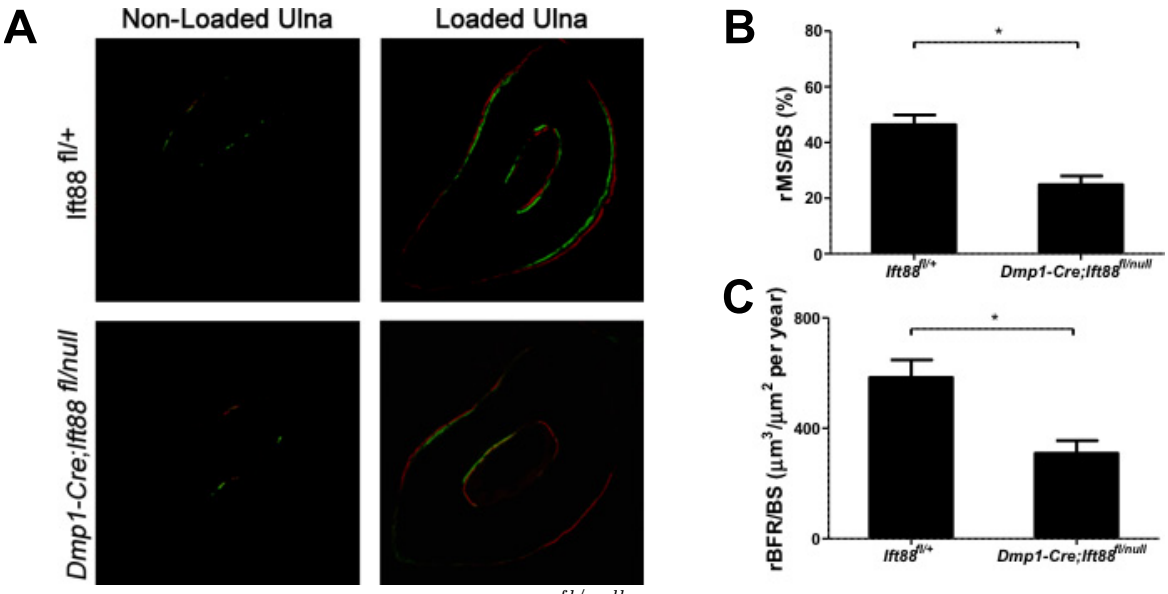

Figure 2.5: Skeletally mature *Dmp1-Cre;Ift88*$^{fl/null}$ mice showed a significantly reduced response to ulnar loading. (A) Representative images of non-loaded (left) and loaded (right) ulnae of *Ift88*$^{fl/+}$ (top) and *Dmp1-Cre;Ift88*$^{fl/null}$ (bottom) mice with fluorochrome labels (Calcein in green and Alizarin Red in red). We measured decreased (B) relative mineralizing surface (rMS/BS) and (C) relative bone formation rate (rMBR/BS) in mice with targeted deletion of *Ift88* in osteocytes. Data presented as mean ± SEM. n = 15 for *Dmp1-Cre;Ift88*$^{fl/null}$ and n = 14 for *Ift88*$^{fl/+}$ groups. * $p < 0.05$.

formation response was reduced in the conditional knockout mice by 46% in rMS/BS and 47% in rBFR/BS (Figure 2.5). We also measured the relative bone formation response in the other genotypes, *Ift88*$^{fl/null}$ and *Dmp1-Cre;Ift88*$^{fl/null}$, and found no difference when compared to our control, *Ift88*$^{fl/+}$ (data not shown). Similarly, we did not find that gender had a significant effect and pooled data across genders for each genotype.

2.5 Discussion

Our data demonstrate *in vivo* for the first time that the osteocyte cilium mediates mechanotransduction in bone. Although this is not the first *in vivo* study on primary cilia in bone, previous studies relied on Cre recombination driven by osteocalcin or Colα1(I) promoters that are expressed in osteoblasts and only one study has investigated the role of cilia in skeletal adaptation [Qiu *et al.*, 2012a; Temiyasathit *et al.*, 2012]. The roles of the osteoblast and osteocyte cilium cannot be distinguished because the recombination in osteoblasts is carried through to osteocytes as those osteoblasts mature. Prior studies also targeted *Kif3a*, which has both ciliary and non-ciliary roles, including Wnt signaling [Corbit *et al.*, 2008].

By demonstrating that ablation of osteocytes inhibited unloading-induced skeletal adapatation, Tatsumi et al. identified osteocytes as the principal mechanosensing cells in bone [Tatsumi *et al.*, 2007]. Since then, studies have continued to support their finding that osteocytes coordinate skeletal adapation in response to changes in the loading environment. For example, osteocytes are strikingly more sensitive to their mechanoenvironment than osteoblasts [Kamel *et al.*, 2010; Santos *et al.*, 2009] and osteocyte apoptsis has been linked to microdamage caused by bone fatigue [Cardoso *et al.*, 2009; Verborgt *et al.*, 2000]. Findings in this study both support the paradigm that osteocytes are the principal mechanostransducing cells in bone and also implicates the primary cilium of the osteocyte in detecting the mechanical load. Strikingly, when comparing this study to that of studies targeting primary cilia in osteocytes and osteoblasts, are remarkably similar to that of studies targeting primary cilia in osteocytes and osteoblasts, the impaired bone formation

response to load is remarkably similar [Qiu *et al.*, 2012a; Temiyasathit *et al.*, 2012]. When compared to the osteoblast cilium, this suggests that the osteocyte primary cilium is the main contributor to loading-induced osteogenesis.

Interestingly, previous studies deleting osteoblast and osteocyte cilia reported reductions in mineral apposition rate, which in turn led to an impaired bone formation. [Qiu *et al.*, 2012a; Temiyasathit *et al.*, 2012]. These data seem to contradict results in this study where reductions in mineralizing surface led to the impaired bone formation. Mineral apposition rate is an indicator of individual cell activity in contrast to mineralizing surface, an indicator of the number of active cells in the remodeling process. This discrepancy may be attributed to the conditional knockout of non-ciliary specific *Kif3a* used in previous studies. Deletion of *Kif3a* has already been demonstrated to affect the Wnt/β-catenin pathway and recently, another study demonstrated that this pathway can mediate mineral apposition rate [Javaheri *et al.*, 2014]. It is possible that *Kif3a* plays a role in two distinct bone formation mechanisms, one involving cilia and one involving the Wnt pathway. By targeting a cilia-specific gene, the data in this study suggest that the osteocyte primary cilium is involved in mediating the number of active cells but not the magnitude of the individual cell's activity in the remodeling process.

In this study, we focused on the role of the osteocyte in bone formation and did not address its role in bone resorption. It is possible that the osteocyte cilium is also involved in the osteocyte's mechanosensing, but we suspect it is through a different mechanism. This difference has been previously observed with β1 integrin. Deleting β1 integrins from cortical osteocytes led to a reduced loading-induced bone formation response and no differences in bone geometry [Litzenberger *et al.*, 2009]. In contrast,

when these mice were hindlimb unloaded, rapid changes in bone geometry occurred and strengthened the bone [Phillips *et al.*, 2008]. Collectively, these studies show that $\beta 1$ integrins play different roles. In skeletal unloading or disuse, $\beta 1$ integrins negatively regulate mechanotransduction while in skeletal loading, they positively regulate mechanotransduction. Here, we show that the osteocyte primary cilium positively regulates skeletal loading. An unanswered question is if osteocyte cilia play a role in detecting the unloading and if deleting osteocyte cilia will positively or negatively mediate the adapation.

It has been previously reported that *Ift88* and *Kif3a* deletion disrupt intraflagellar transport but this disruption may not inhibit cilia formation. Cilia are formed when cells are arrested in interphase and are resorbed during mitosis [Kobayashi and Dynlacht, 2011; Quarmby and Parker, 2005; Wheatley *et al.*, 1996]. It is possible that the osteocyte cilium is formed when the cell was an osteoblast and the cilium is retained through the terminal differentiation. However, by staining for the cilium *in situ*, our data shows that deleting *Ift88* led to decreased incidence of cilia. Combined with our data showing this deletion was targeted specifically to osteocytes, this study demonstrates that conditionally deleting *Ift88* using the *Dmp1* promoter prevents cilia formation in osteocytes. This did not prevent all osteocyte cilia from forming, 25% of *Ift88* expression remained and some cilia were still observed. The remaining *Ift88* expression may be explained by the isolation technique resulting in only an enrichment of osteocytes to approximately 70% [Stern *et al.*, 2012]. Although the presence of non-osteocytes in the cell population may explain the remaining *Ift88* expression *in vitro*, this is a less likely explanation for the presence of cilia *in situ*, where osteocytes are the predominant cell type accounting for nearly 95% of cells in bone [Bonewald, 2011]. We attribute the remaining

incidence of cilia *in situ* and expression of *Ift88 in vitro* to incomplete recombination. The variable effectiveness of Cre has been reported by others [Araki *et al.*, 1997; Xiao *et al.*, 2010]. Even with the incomplete Cre recombination, it was sufficient to lead to a marked impairment in skeletal adaptation.

With the potential variation in Cre effectiveness, we generated *Dmp1-Cre;Ift88*$^{fl/null}$ mice instead of *Dmp1-Cre;Ift88*$^{fl/fl}$ mice. With a null allele, Cre recombination only needs to occur with one floxed allele. With two floxed alleles, the Cre must recombine both alleles, exacerbating the potential issue of partial Cre acitivity. This led to three possibilities for controls *Ift88*$^{fl/+}$, *Ift88*$^{fl/null}$ and *Dmp1-Cre;Ift88*$^{+/null}$ genotypes. We examined bone architecture between all three genotypes and because we found no differences in skeletal morphology, we reduced our comparisons and selected one control, *Ift88*$^{fl/+}$.

We did not find any measureable differences in skeletal morphology with deletion of Ift88 in osteocytes, suggesting osteocyte cilia are not involved in skeletal development. This supports previous findings from another study in our lab [Temiyasathit *et al.*, 2012]. Because we only analyzed 16-week-old mice, it is possible that impairment in skeletal development may have already been corrected. This has been reported in a bone-specific deletion of *Kif3a*, where an osteopenic phenotype at 6 weeks was corrected by 24 weeks [Qiu *et al.*, 2012a]. In other studies, a bone-specific deletion of *Pkd1* and a global inactivation of a *Pkd1* allele led to a measureable deficits in skeletal developments [Qian *et al.*, 2005; Xiao *et al.*, 2011; Xiao *et al.*, 2010]. The *Kif3a* findings are not surprising because it has been linked to Wnt/β-catenin pathway, known to regulate skeletal development. Disruption of the pathway can impair skeletal development [Day *et al.*, 2005; Galli *et al.*, 2010;

Holmen *et al.*, 2005; Kramer *et al.*, 2010; Tu *et al.*, 2012]. In contrast, Polycystin 1, the protein encoded by *Pkd1*, is expressed throughout the cell [Kodani *et al.*, 2013; Yoder, 2002] and through differentiation of chondrocytes and osteoblasts [Lu, 2001]. Measurable effects may be expected with deleting a gene that is so extensively expressed. Thus the abnormal skeletal morphology observed with the global inactivation of a single allele of *Pkd1* is not surprising [Xiao *et al.*, 2011; Xiao *et al.*, 2010]. Finally, our report of changes in skeletal remodeling but not development is not uncommon with transgenic mouse models. For example, other models reporting impaired skeletal adapation but normal development include osteopontin [Ishijima *et al.*, 2001], β1 integrin [Litzenberger *et al.*, 2009; Phillips *et al.*, 2008], and adenylyl cyclase 6 [Lee *et al.*, 2014]. Other groups have reported that IFT is necessary for normal skeletal development, but in those mouse models, IFT was impaired globally or early in a cell lineage [Haycraft *et al.*, 2007; Murcia *et al.*, 2000; Song *et al.*, 2007; Zhang *et al.*, 2003], which extensively affects IFT. While it is possible that the osteocyte cilium has a role in skeletal development, we found that it is not to a measureable extent.

Though the impairment in bone formation was striking, this conditional deletion did not completely inhibit the bone formation response to load. We can attribute any remodeling in the skeleton as a response to load because the murine skeleton does not normally remodel [Jerome and Hoch, 2012]. The remaining bone formation response may be attribute to other cellular mechanosensors. Candidate mechanosensors in the osteocyte that have been proposed include the cilium, the cytoskeleton, dendritic processes, and several membrane proteins [Burra *et al.*, 2010; Cheng *et al.*, 2001; Cherian *et al.*, 2005; Xiao *et al.*, 2011; Xiao *et al.*, 2006; You *et al.*, 2001]. While we report a significant decrease in loading-induced bone

formation with loss of osteocyte cilia, the remaining bone formation may be attributed to other mechanosensing domains of the osteocyte.

Here, we studied the osteocyte cilium in vivo and present for the first time direct evidence connecting the osteocyte cilium to skeletal adaptation. Our data show that conditional deletion of *Ift88* in osteocytes disrupts cilia formation and results in impaired loading-induced bone formation. The cilium continues to emerge as a mechanosensing organelle across a breadth of tissue and cell types. Within bone, the osteocyte cilium has become increasingly implicated. Elucidating the mechanisms through which osteocyte cilia mediate bone mechanotransduction will enable this organelle as a new target for treatments of bone loss disorders.

Chapter 3

Lateral visualization of the cilium in assessing protein function

Collaborators on this project are Kristen L. Lee, Marie D. Gueverra, and Christopher R. Jacobs.

3.1 Abstract

Proteins localizing to the cilium are often, not surprisingly, critical to ciliary function. Immunocytochemistry is an important technique used not only to demonstrate localization of a protein to the cilium but also in determining its role in ciliary function. The ciliary localization of some proteins can be easily visualized by traditional epifluorescence microscopy. In contrast, this method can fail to detect the ciliary localization of other proteins due to the interference by the cell body. This can then result in an inaccurate and misleading conclusion that a protein is absent from the cilium. In this study, we classify ciliary localization of proteins as exclusive, enhanced and inconclusive localization. We then stain MLO-Y4 osteocyte-like cells for ADP-ribosylation factor-like protein 13b, Polycystin 2 and Piezo1 to present examples each classifications, respectively. Visualizing the immunostaining laterally enabled a clear distinction between the ciliary and cytoplasmic localization of Piezo1. Apical-basal imaging alone may have erroneously excluded this protein from the cilium. Strikingly, we found 15 out of 23 papers assessing ciliary localization had excluded proteins soley based on apical-basal imaging. Here, we show the importance of lateral imaging to confidently exclude proteins from the cilium.

3.2 Introduction

Cilium-specific and nonspecifically-localized proteins are found in the primary cilium. Often these proteins are crucial to the cilium's chemosensory and mechanosensory roles. For example, Patched-1 is a receptor in the Hedgehog signaling pathway, a pathway important in development and its localization to the cilium can inhibit the pathway [Rohatgi *et al.*, 2007]. Polycystin-1 and Polycystin-2 (PC1/2) form the polycystin complex that mediates the calcium response in ciliary mechanosensation [Nauli *et al.*, 2003]. ADP-ribosylation factor-like protein 13b (Arl13b), implicated in a known ciliopathy Joubert Syndrome, is important for cilia formation and neuron development as well as the previously mentioned Hedgehog signaling pathway [Higginbotham *et al.*, 2012; Larkins *et al.*, 2011]. Co-immunostaining for candidate proteins and cilia to determine whether a protein localizes to the cilium compartment is an important step in examining a protein's role in ciliary function. Assessing this immunostaining with epifluorescence microscopy results in three classifications: exclusive, enhanced, and non-distinguishable localization (Figure 3.1).

Some proteins can be easily determined to localize to the cilium with traditional epifluorescence microscopy . However this method can also fail to detect other proteins that nonspecifically localize to the cilium and are found throughout the cell. For example, isoforms of adenylyl cyclases (AC2-5, AC7), Nephronophthisis 9 in inversin-deficient cells, and PC1 in Bardet-Biedl syndrome 1-deficient cells were not found in the ciliary compartment with apical-basal imaging [Choi *et al.*, 2011; Kwon *et al.*, 2010; Shiba *et al.*, 2010; Su *et al.*, 2014]. Others have reported proteins

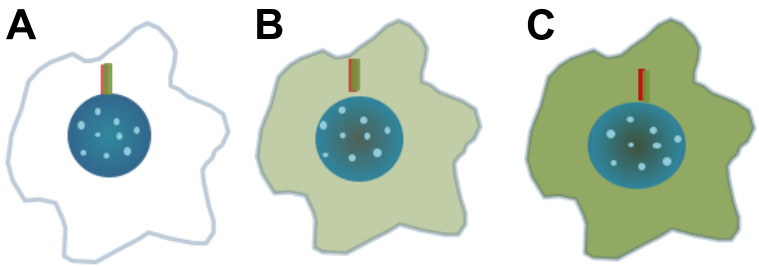

Figure 3.1: Classifications of ciliary protein localization. A) Exclusive localization to the cilium, B) Enhanced, such that the cilium is distinguishable from the cell body, and C) Inconclusive. Cell nucleus is depicted in blue, cilium in red, and protein of interest in green.

were absent from the ciliary compartment in protein trafficking studies which required 3-D reconstruction of apical-basal images [Berbari *et al.*, 2008; Corbit *et al.*, 2005; Geng *et al.*, 2006]. Here, our goal was to identify cases when apical-basal imaging was and was not sufficient to distinguish protein localization to the ciliary and cytoplasmic compartments. Apical-basal and lateral images were compared of cells after staining for ciliary marker acetylated α-tubulin and proteins of interest, Arl13b, PC2, or Piezo1.

3.3 Methods

MLO-Y4 osteocyte-like cells were cultured as previously described [Kwon *et al.*, 2010; Malone *et al.*, 2007]. Briefly, coverslips were coated with collagen and seeded with cells at 4,000 cells/cm^2. Cells were cultured in serum-reduced media (2.5% FBS, 2.5% CS) for 2 days and then fixed in 10% formalin. Cells were stained using primary antibodies targeted against acetylated α-tubulin (Abcam, ab24610, 1:1000) and Arl13b (ProteinTech, 17711-1-AP, 1:1000), PC2 (Santa Cruz, sc-25749, 1:500), or Piezo1 (Novus, NBP1-78537, 1:25) followed by appropriate fluorescently-tagged secondary antibodies. Z-stacks at 0.2 μm-thick intervals of immunostained cells were captured by a laser scanning confocal microscope (Leica TCS SP5) with a 100$\times$ objective (1.46 NA, oil immersion). These were used in a maximum projection to generate apical-basal images as well as reconstructed laterally using the Leica Application Suite.

3.4 Results

Signal from the cell body can overwhelm signal from the cilium and potentially interfere with visualizing the cilium when imaged in the apical-basal direction. This can be addressed by also imaging or reconstructing an image laterally. Using multiple axes to examine immunocytochemistry samples enables ciliary and cytoplasmic signals to be clearly visualized. Without this additional examination, proteins can be incorrectly determined to be absent from the cilium. In some cases this additional step is not necessary. For example, Arl13b and PC2 are easily determined to localize to the cilium with apical-basal images (Figures 3.2a,b). In contrast, apical-basal images of Piezo1 staining suggest that was only present in the cytoplasmic compartment (Figure 3.2c). Examining the lateral images shows that Piezo1 is also present in the ciliary compartment (Figure 3.3). We then reviewed 23 articles reporting ciliary localization of proteins and remarkably found 15 articles, including our own, have excluded proteins from the cilium without lateral imaging (Table 3.1).

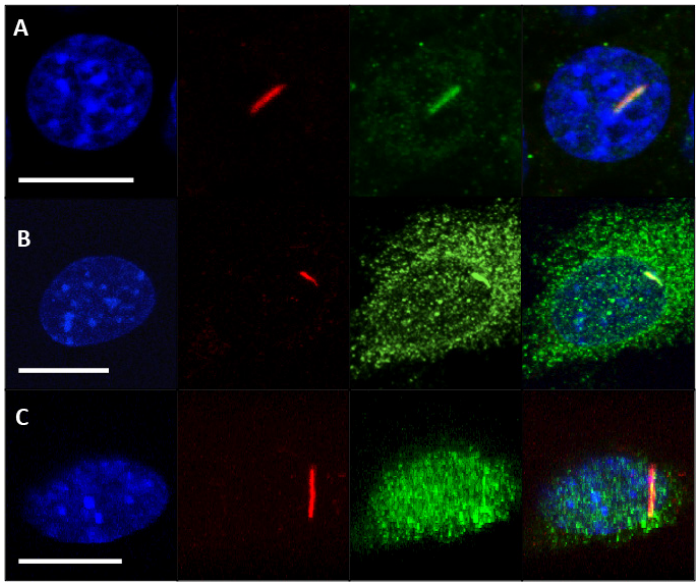

Figure 3.2: Apical-basal images of immunocytochemistry. A) Arl13b has exclusive localization and B) PC2 has enhanced localization, while C) Piezo1 has non-distinguishable localization. Cells were stained for DAPI (blue), acetylated α-tubulin (red), and the protein of interest (green). Scale bar indicates 10 μm.

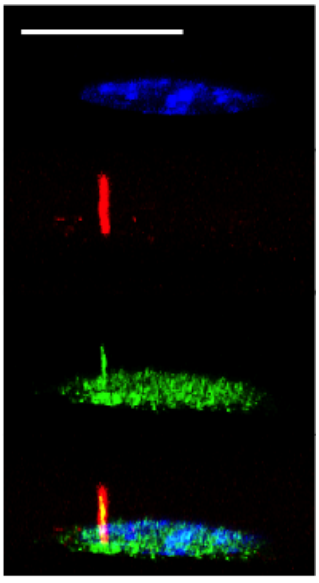

Figure 3.3: Lateral images of Piezo1 immunostaining in MLO-Y4 cells. Cells were stained for DAPI (blue), acetylated α-tubulin (red), and Arl13b (green). Scale bar indicates 10 μm.

Findings	Reference
With corresponding lateral and apical-basal imaging	
Somatostatin receptor 1,2,4,5 and Serotonin receptor 7 were excluded from cilium	[Berbari *et al.*, 2008]
Smoothened localization is mediated by Hedgehog signaling	[Corbit *et al.*, 2005]
Mutations and select fragments of Polycystin 2 sequence and human transferring receptor do not localize to the cilium	[Geng *et al.*, 2006]
Retinitis pigmentosa 2 localization is mediated by Importin β2	[Hurd *et al.*, 2011]
Select fragments of Cystin sequence in a GFP do not localize to the cilium	[Tao *et al.*, 2009]
Mutations of Polycystin 1 sequence were excluded from the cilium	[Ward *et al.*, 2011]
Polycystin 1 in human renal cyst epithelial cells has reduced localization to the cilium	[Xu *et al.*, 2007]
Polycystin 1 in Oak Ridge polycystic kidney cells has reduced expression along the cilium	[Yoder, 2002]
With apical-basal imaging only	
Phosophodiesterase 4C localization required hepatocyte nuclear factor-1β	[Choi *et al.*, 2011]
Identification of fibrocystin's ciliary targeting sequence	[Follit *et al.*, 2010]
Targeting of inositol polyphos- phate-5-phosphatase E to the cilium required Arl13b, prenyl-binding protein phosphodiesterase 6D and centrosomal protein 164	[Humbert *et al.*, 2012]
Enrichment of cyclic nucleotide-gated channel A2 requires B1b	[Jenkins *et al.*, 2006]
Adenlyl cyclase 2-5 and 7 do not localize to the cilium	[Kwon *et al.*, 2010]
ADP-ribosylation factor domain does not localize to the cilium	[Larkins *et al.*, 2011]
Mutations of neuropeptide Y2 receptor prevent localization	[Loktev and Jackson, 2013]
Gαs was excluded from the cilium	[Masyuk *et al.*, 2013]
Mutations of collapsing response mediator 2's sequence prevented localization to the cilium	[Ou *et al.*, 2012]
Proteolytically processed forms of Gli2 do not localize to the cilium	[Santos and Reiter, 2014]
Smoothened localization was mediated by Bardet-Biedl Syndrome proteins and Leucine-zipper transcription factor-like 1	[Seo *et al.*, 2011]
Inversin mediates localization of products of Nephronophthisis type 3 and 9	[Shiba *et al.*, 2010]
Bardet-Biedl syndrome protein 1 was required for Polycystin 1 localization	[Su *et al.*, 2014]
Mutations in Nephronophthisis type 9 prevented localization to the cilium	[Trapp *et al.*, 2008]
Small molecules inhibited ciliary localization of Smoothen	[Wu *et al.*, 2012]

Table 3.1: Findings on protein localization that have been drawn with and without lateral imaging.

3.5 Discussion

The primary cilium is intrinsically difficult to visualize. Relative to the cell body, the cilium is a mere 1/30,000 of the cell volume [Mitchell *et al.*, 2009]. Not only is this organelle small, it can vary in length from 0.2 to over 10 μm [Mitchell *et al.*, 2009; Uzbekov *et al.*, 2012] and adopt a variety of orientations with respect to the cell body [Choi *et al.*, 2011]. Not surprisingly, even with advanced techniques, imaging this organelle is challenging [Wheatley and Bowser, 2000].

For many proteins, ciliary localization can be easily confirmed with traditional epifluorescence microscopy. However, we show that to determine that a protein does not localize to the cilium requires visual assessment along multiple axes. Strikingly, numerous studies have excluded proteins from the ciliary compartment without a thorough assessment and these proteins ma need to be revisited. Determining whether a protein is present or absent from the cilium is an integral step in assessing the cilium as a complex and multifunctional organelle. For example, protein localization is important in identifying new signal transduction pathways mediated by the cilium, relating novel mutations to ciliopathies, and directing therapies to the ciliary compartment. Future studies will continue to improve the efficiency and accuracy in assessing protein localization, a critical component to understanding the cilium.

Chapter 4

Primary cilia mechanosensation adapts and regulates cell signaling

Collaborators on this project are Yuan N. Young and Christopher R. Jacobs.

4.1 Abstract

A cell's ability to sense its mechanoenvironment, or mechanosensing, is critical to its survival. Often the mechanoenvironment can condition cellular sensors and their adaptation allows them to function in diverse environments. Strikingly, though sensory adaptation is crucial, the mechanisms responsible are poorly understood. Primary cilia have recently emerged as mechanosensors that can deflect in response to its mechanoenvironment. In this study, we demonstrate cilium stiffness can be modulated mechanically and chemically. Exposure to fluid flow stiffens the cilium, resulting in smaller deflections to later exposures. Increasing acetylation also stiffens the cilium and this acetylation-induced stiffening decreases cellular responsiveness to mechanical stimuli. Collectively, our data demonstrate the cilium is a cellular mechanosensor with the capacity to adapt and regulate cellular sensitivity to its mechanoenvironment.

4.2 Introduction

Sensing and responding to physical cues are critical cellular processes within living organisms. Their dysfunction can result in diseases, including atherosclerosis, osteoporosis, and cancer [Hoffman *et al.*, 2011], and cells become bombarded by stimuli. For example, blood flow becomes disturbed with atherosclerosis, tissue resorption occurs with osteoporosis, and tissue increasingly stiffens with tumor progression. These cells must respond and adapt to their changing mechanoenvironment in order to survive and maintain homeostasis. We introduce the term sensory adaptation to describe a cellular sensor's adjustment to its surrounding environment, allowing a sensor to operate in response to diverse stimuli [Kurahashi and Menini, 1997]. One example of sensory adaptation is the bacterial mechanosensitive channel that prevents a cell from rupturing when exposed to extreme osmotic stress. These channels can be desensitized or inactivated when exposed to a sub-threshold level of stress [Anishkin and Sukharev, 2009]. Sensory adaptation in mammalian cells has been best studied in specialized sensory cells, including those of auditory, olfactory and retinal systems [Condon and Weinberger, 1991; Kurahashi and Menini, 1997; Pugh *et al.*, 1999]. The ligand-gated channels of olfactory sensory cells are involved in the chemosensing response to odorant stimuli and can alter its ligand affinity in response to stimuli [Kurahashi and Menini, 1997]. Strikingly, no clear mechanism has been identified in sensory adaptation even in its most studied context of the bacterial mechanosensitive channels and the evidence for adaptation remains disputed [Naismith and Booth, 2012].

In addition to ion channels, the most characterized and understood type of

mechanosensors [Hirata *et al.*, 2014], cells can sense physical cues through non-channel mechanosensors. A subset of non-channel mechanosensors are structural mechanosensors, cellular sensors that bear load as well as detect mechanical stimuli. For example, focal adhesions and the cytoskeleton can function as structural mechanosensors and have previously been shown to adapt. After mechanical stimulation, focal adhesions, for example, have been shown to enlarge and thicken due to recruitment of vinculin [Galbraith *et al.*, 2002]. Though vinculin is thought to reinforce focal adhesions, this has not been demonstrated experimentally. It also has not been determined whether vinculin recruitment regulates cellular responsiveness.

In this study, we demonstrate that the primary cilium is a mechanosensor that adapts and identify a mechanism through which the cilium can regulate cellular responsiveness to mechanical stimuli. The cilium has been suggested to have the ability to adapt as a mechanosensor and regulate cellular responsiveness. Cilium deflection is transduced to a cyclic AMP signaling response [Besschetnova *et al.*, 2010; Kwon *et al.*, 2010] and this response has been associated with regulating cilium length [Besschetnova *et al.*, 2010; Ou *et al.*, 2009]. Longer cilia are thought to be more sensitive to mechanical stimuli [Besschetnova *et al.*, 2010; Rydholm *et al.*, 2010]. Collectively, these data present one mechanism, length, that the cilium can adapt and affect cellular responsiveness.

4.3 Methods

4.3.1 Cell culture

Mouse inner medullary collecting duct (IMCD) cells transfected with live cell ciliary marker somatostatin receptor 3 fused to GFP (gift of Bradley K. Yoder of University of Alabama at Birmingham) were cultured on fibronectin-coated coverslips and slides in growth medium (DMEM F-12 with 10% FBS, 1% P/S and 200 μg/mL geneticin). At 70% confluence, cells were serum-starved for 72 hours (0% FBS) to promote cilia formation. For the tubacin experiment, cells were cultured as described above and treated with 0.5 mM of tubacin or niltubacin (Enzo Life Sciences, Farmingdale, NY) for 4 hours prior to exposure to flow. For the *HDAC6* knockdown experiment, cells were cultured to 60% confluence in growth media and transfected with scrambled control or *HDAC6* siRNA (sc35545; Santa Cruz Biotechnology, Dallas, TX) using Lipofectamine 2000 (Life Technologies, Carlsbad, CA). Cells were serum-starved the following day for 72 hours and then used in flow experiments.

4.3.2 Fluid flow

For cilium deflection studies, cells seeded on coverslips were mounted in a laminar flow chamber (RC-30; Warner Instruments, Hamden, CT). Steady flow at a rate of 0.5 mL/min, corresponding to 0.25 Pa of wall shear stress used in previous studies [Downs *et al.*, 2012; Young *et al.*, 2012], was applied with a syringe pump (GeniePlus; Kent Scientific, Torrington, CT) and a 10 mL syringe (Norm-Ject; Air-

Tite, Virginia Beach, VA). Flow medium used was DMEM F-12 without phenol red. For the 2-minute bouts of flow, flow was applied for 2 minutes, stopped for 2 minutes and applied for another 2 minutes. For the 10 minute bouts, flow was applied for 10 minutes, stopped for 2 minutes and applied for an additional 10 minutes.

For gene expression studies, cells seeded on slides were mounted in large parallel plate flow chambers as previously described [Jacobs *et al.*, 1998]. Briefly, after slides were placed in each flow chamber, incubated for 30 minutes and exposed to 1 hour of oscillatory fluid flow at 1 Hz with a peak shear stress of 1 Pa. Flow parameters were chosen to correspond to a previous study finding an increase in microtubule density at the cilium base with flow [Espinha *et al.*, 2014]. Immediately after exposure to flow, slides were washed with PBS and cells were lysed for RNA extraction.

4.3.3 Imaging and post-processing

A high-speed laser scanning confocal microscope with a 16 Hz bi-directional resonant scanner and a 100× oil objective (1.46NA) was used to collect 3D images of primary cilia (512x512 z-stacks, TCS SP5; Leica Microsystems, Buffalo Grove, IL). Each z-stack was acquired in approximately 3 seconds. Cilia can be visualized with fluorescence microscopy due to the somatostatin receptor 3 GFP fusion protein targeted to the organelle (Excitation: 488nm, Emission: 509 nm). Images were post-processed as previously described [Downs *et al.*, 2012; Young *et al.*, 2012]. Briefly, a Gaussian filter was applied followed by a threshold. To determine the center of the cilium within each slice of the z-stack, the x and y coordinates of the pixels with an intensity value above the threshold were averaged.

4.3.4 Deflection analysis

The model used to approximate cilium mechanics is described in detail in a previous paper, where the cilium is represented as a cylindrical elastic beam coupled to a rotational spring under hydrodynamic load [Young *et al.*, 2012]. Briefly, the cilium coordinates at rest and under flow were normalized by the length of the cilium and parameterized as a function of the position along the cilium. The observed cilium profile is fit to the deflection predicted by the model using the method of least squares and varying mechanical properties. Specifically, the cilium profile at rest is used to determine the internal stress within the cilium. The cilium profile with flow at 30 seconds, 2 minutes or 10 minutes is used to extract stiffness at those time points.

4.3.5 mRNA expression

RNA was extracted from cell lysate using the Autogen RNA Extraction kit and the Quickgene Mini80 (Autogen; Holliston, MA). The TaqMan reverse transcription kit (Life Technologies) was used for reverse transcription. Samples were analyzed in triplicate by relative quantitative real-time RT-PCR and expression was normalized to that of housekeeping gene *GAPDH*. Relative quantification of expression levels was determined using the standard curve method with the following primer-probe pairs: *HDAC6* (Mm01341125_m1), *COX-2* (Mm00478374_m1), and *GAPDH* (4352339E).

4.3.6 Immunocytochemistry

Cells were fixed in 10% formalin and permeabilized with 0.1% Triton-X. Cells were then incubated in primary antibody solution, anti-acetylated α-tubulin (Abcam, 6-11B-1, 1:1000), and the secondary antibody solution, anti-mouse Alexa Fluor 568 (Life Technologies, 1:200). Cells were imaged on a laser scanning confocal microscope (Leica SP5; Leica Microsystems, Buffalo Grove, IL) with a 63x oil objective (1.4NA). Maximum-intensity z-projections were generated with the Leica software.

4.3.7 Western blots

Cells were lysed in radioimmunoprecipitation (RIPA) buffer (Thermo Scientific; Waltham, MA) and protein content was measured by bicinchoninic acid assay. Protein was separated by electrophoresis in 4-12% Bis-Tris polyacrylamide gels (NuPage, Life Technologies) and transferred to polyvinyl difluoride membranes. Membranes were probed for acetylated α-tubulin (6-11B-1, 1:1000; Abcam, Cambridge, MA) and actin (AC-40, 1:2000; Abcam). The bound primary antibodies were detected by chemiluminescence with HRP-conjugated secondary antibodies (1:10000; Millipore, Billerica, MA).

4.3.8 Statistical analysis

All data are presented as mean $\pm$ SEM and analyzed with GraphPad Prism (GraphPad Software, Inc., La Jolla, CA). A one-way repeated measures ANOVA was

used to assess the effects of duration of flow exposure on cilium stiffness with a Dunn's post hoc test for multiple comparisons. A two-way ANOVA was used to assess effects of siRNA-mediated knockdown and flow on mRNA expression followed by Sidak's multiple comparisons test. Statistical significance was considered at $p < 0.05$.

4.4 Results

In a previous study, we reported that cilia deflected by a bout of flow often failed to recover to their original positions [Downs *et al.*, 2012]. This suggested the cilium could adapt structurally to flow. We hypothesized that this was a feature of the cilium's sensory adaptation and the cilium may alter its mechanical properties in response to stimuli. First, we determined ciliary biomechanics by examining changes in cilium deflection with exposure to flow. To do this, we capture the cilium's 3D position at rest and under flow (Figure 4.1A) and use a computational model to determine its mechanical properties [Young *et al.*, 2012]. We found that after exposure to 2 minutes of flow the cilium stiffens along the axoneme and at the base, 2.6 ± 0.7 and 3.3 ± 0.6 times (n = 6, Figure 4.1B,C), respectively. Next, we applied longer bouts of flow for 10 minutes and also found cilia stiffened 1.8 ± 0.4 times along the axoneme and 4.0 ± 1.5 times at the base (n = 6, Figure 4.1B,C). Interestingly, longer exposure to flow did not further stiffen cilia. This suggests that adaptation process is completed on a short time scale. We also examined the cilium's resting position before and after flow, introducing the cilium's protrusion angle to describe the angle between the cilium and the cell (Figure 4.1A). We confirmed prior observations that the cilium rotates with flow [Downs *et al.*, 2012]. The protrusion angle decreased 3.9 ± 0.6° with flow (Figure 4.1D). These data show the cilium can adapt to flow by altering its stiffness and orientation. Interestingly, these adaptations occurred on a time scale of minutes in contrast to the 3 hours for flow-induced changes in cilium length previously reported [Besschetnova *et al.*, 2010]. We did not find any changes in cilium length, suggesting that cilium adapts over diverse time scales and mechanisms. This may explain this organelle's multifunctionality and ability to operate in such a

range of mechanoenvironments.

After finding that the cilium's mechanical properties can be modulated, we suspected these adaptations may be driven in part by biochemical processes. Microtubule doublets form the cilium's axoneme and give the cilium its structural integrity [Schwartz *et al.*, 1997]. In single microtubule studies, groups have reported changes in stiffness with post-translation modifications of microtubules, including acetylation [Felgner *et al.*, 1996; Hawkins *et al.*, 2013]. Interestingly, acetylation has been shown to increase in response to mechanical stimuli [Geiger *et al.*, 2009; Li *et al.*, 2011]. This suggests that adaptation occurs through a mechanism involving acetylation. We hypothesized cilium stiffness may also be modulated by an acetylation-mediated mechanism. To examine this, we used tubacin, a potent pharmacological deacetylation-inhibiting agent. In contrast to other inhibitors can also affect chromatin acetylation, tubacin binds the α-tubulin domain of histone deacetylase 6 (HDAC6) and only affects tubulin acetylation [Haggarty *et al.*, 2003]. We treated IMCD cells with tubacin or niltubacin, an inactive analogue, and exposed them to flow. We found cilia stiffened 4.0 $\pm$ 1.3 times along the axoneme with tubacin (n = 5 per group, Figure 4.2A) and verified the increased acetylation with immunocytochemistry and western blot (Figure 4.2B,C). These data show that increasing tubulin acetylation can stiffen the cilium and present a possible mechanism for the cilium to modulate its mechanical properties.

We next hypothesized that the cell's internal mechanisms to regulate acetylation were sufficient for ciliary stiffening. We transfected IMCD cells with siRNA against *HDAC6*, which encodes a microtubule-associated deacetylase [Haggarty *et al.*, 2003], or with a scrambled control. We found a 2.7 $\pm$ 0.9 fold increase in ciliary stiffness

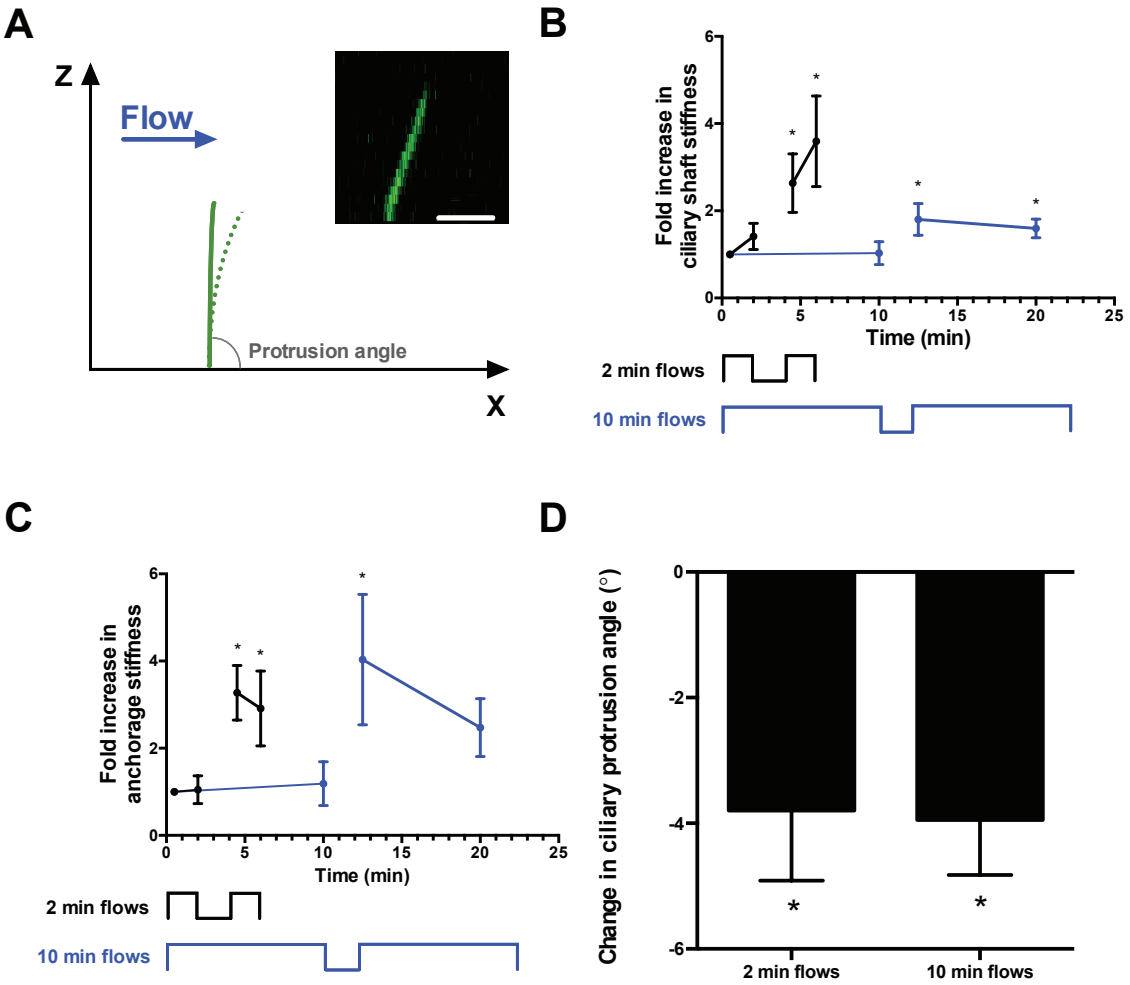

Figure 4.1: Flow stiffens and repositions primary cilia. (A) Schematic depicting a cilium at rest (solid green line) and deflecting with flow (dashed green line) with a representative fluorescence micrograph from which cilium position is determined (inset). The x-axis is positioned at the junction of the cilium and the cell and the protrusion angle measures the orientation of the cilium with respect to the cell. Scale bar indicates 2.5 μm. (B) Cilia were exposed to 2-minute (black) or 10-minute (blue) bouts of flow separated by 2 minutes of rest. Bending stiffness of the cilium shaft was measured and normalized to the first measurement at 30 seconds (* denotes significant difference, $p < 0.05$, $n = 6$ per group). Stiffness increased with exposure to flow, but the increase is independent of duration of flow exposure. (C) Similarly, torsional stiffness anchoring the cilium increased after each rest period independently of flow exposure. (D) The resting position of the cilium with respect to the cell is reported as protrusion angle. The position changes with exposure to flow, decreasing the angle between the cilium and the cell membrane. * denotes significant difference from initial resting position of cilium, $p < 0.05$, ($n = 6$ per group). Data presented as mean ± SEM.

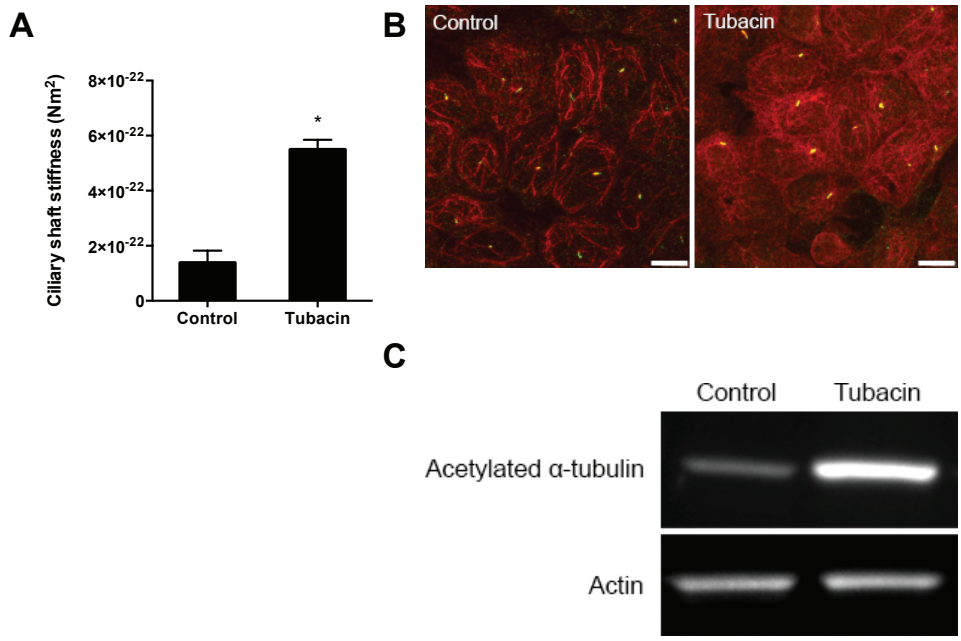

Figure 4.2: Acetylation stiffens primary cilia. (A) Ciliary bending stiffness calculated for the cells treated with niltubacin (control) and tubacin. Tubacin treatment increased rigidity by 4-fold. Data presented as mean ± SEM (n = 5 per group). * denotes $p < 0.05$. (B) Immunostaining against acetylated α-tubulin (red) with cilia marked by SSTR3-GFP (green). The widespread and strong increase staining indicates increase in acetylation. Scale bar indicates 10 μm. (C) Protein expression of acetylated α-tubulin and actin was measured with western blot. Consistent actin bands show the same amount of protein was loaded while strong acetylated α-tubulin band with tubacin treatment confirms increased acetylation previously shown with immunocytochemistry.

with *HDAC6* knockdown (n = 5 per group, Fig. 4.3A). We confirmed the knockdown with real-time quantitative reverse transcription PCR and found a 30.5 ± 8.9% decrease in *HDAC6* expression (n = 10 per group, normalized by housekeeping gene *GAPDH* expression, Fig. 4.3B). While not a complete knockdown, we still observed increased acetylation with immunocytochemistry and western blots (Figs. 3C,D) and not surprisingly, siRNA-mediated acetylation was more modest and less uniform when compared to tubacin-mediated acetylation. These data show that the cell's endogenous regulation of acetylation can modulate cilium stiffness, indicating a specific mechanism for the cell to adapt cilium-mediated mechanosensing.

Given acetylation can stiffen the cilium, we hypothesized a cellular process can allow the cell to internally regulate acetylation and in turn, the cilium as a mechanosensor. We examined this with a siRNA-mediated knockdown of *HDAC6*. We found cilia from knockdown cells stiffened 2.7 ± 0.9 times when compared to cilia of cells transfected with scramble control (n = 5 per group, Figure 4.3A). We analyzed gene expression and measured a knockdown of 30.5 ± 8.9% in *HDAC6* expression (n = 10 per group, normalized by housekeeping gene GAPDH expression, Figure 4.3B). While this was a modest knockdown, it was sufficient to increase cilium stiffness and acetylation (Figure 4.3C,D). Together, these data demonstrate the cell's internal mechanisms to regulate acetylation can also regulate cilium stiffness.

Finally, we determined if these acetylation-induced changes also affect cellular responsiveness. Cyclooxygenase-2 (COX-2) is an inducible enzyme that can be regulated by flow [Flores *et al.*, 2012] and is implicated in increasing renal blood flow as well as the glomerular filtration rate [Harris, 2006]. Because of its role in renal hemodynamics, we used *COX-2* expression to indicate a cell's responsiveness to flow

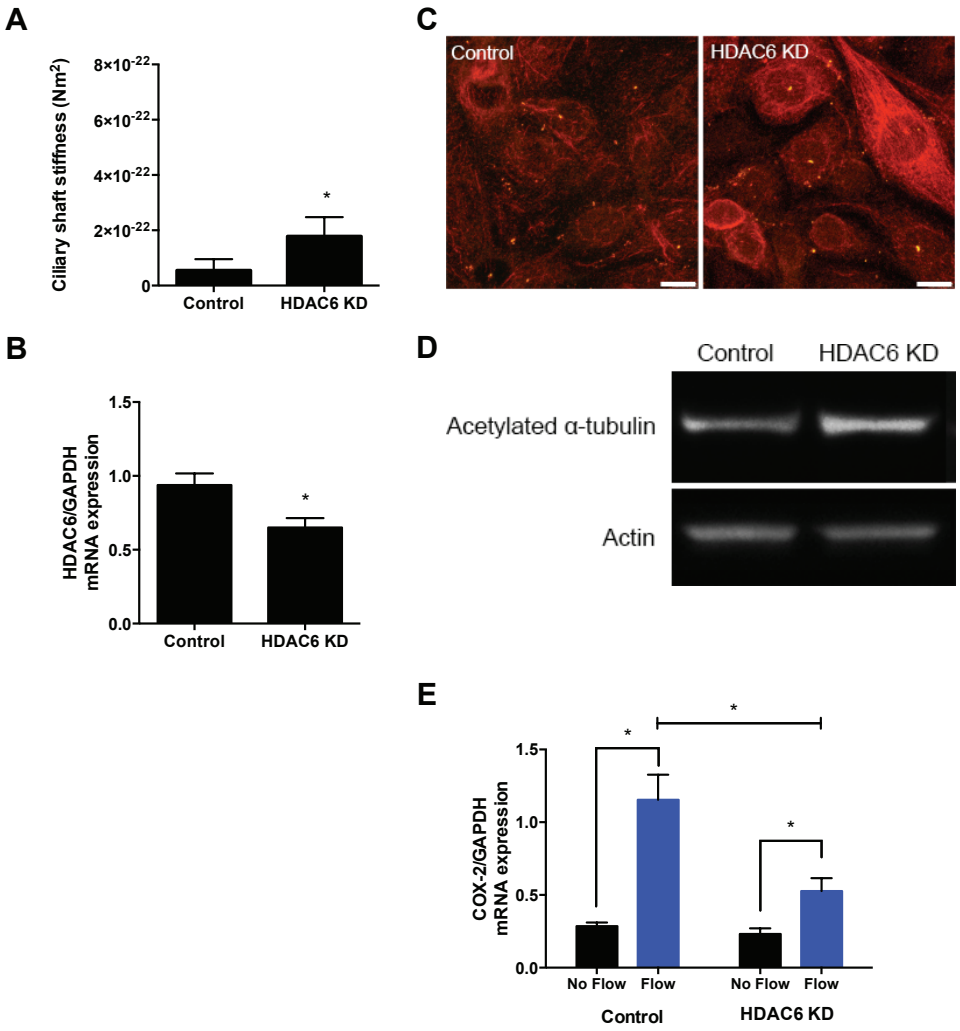

Figure 4.3: The cell's internal mechanism to regulate acetylation can alter cilium stiffness and decrease mechanosensitivity. (A) Cilium stiffness was measured in cells transfected with *HDAC6* siRNA and scrambled control. Knockdown of *HDAC6* resulted in a 3-fold increase in stiffness. (B) *HDAC6* mRNA expression normalized by housekeeping gene *GAPDH* was measured by qPCR in control and knockdown cells. Transfection resulted in a limited knockdown in *HDAC6* mRNA expression. (C) Immunocytochemistry with acetylated α-tubulin staining (red) and SSTR3-GFP cilia marker (green). Increased acetylated α-tubulin staining is observed in some cells. Scale bar indicates 10 μm. (D) Western blot probing for acetylated α-tubulin and actin. The stronger acetylated α-tubulin band in the knockdown cells confirms increased acetylation. (E) *COX-2* expression measured by qPCR with and without flow in cells transfected with *HDAC6* siRNA and scrambled control. A reduction of flow-induced increase in *COX-2* expression is indicative of reduced cell responsiveness with increased acetylation. Data presented as mean $\pm$ SEM (n = 5 per group). * denotes $p < 0.05$.

as an indicator of responsiveness to flow. We exposed cells transfected with HDAC6 siRNA to oscillatory fluid flow and knockdown of *HDAC6* inhibited flow-induced increases in COX-2 expression by 55.9 ± 16.3% (n = 5 per group, normalized by housekeeping gene *GAPDH* expression, Figure 4.3E). Collectively, our data show acetylation modulates cilium stiffness and overall cellular responsiveness to flow.

4.5 Discussion

Here, we propose an acetylation-mediated mechanism that stiffens the cilium in response to mechanical stimuli and regulates cellular mechanosensitivity. When the cilium is bent with flow, acetylation increases, stiffening the microtubule-based axoneme. Strengthening the axoneme results in smaller deflections to future exposures to flow, which reduces the cell's overall responsiveness to flow. Though our data does not directly connect changes in acetylation with flow-induced deflection, decreases in HDAC6 activity and increases in acetylation with mechanical stimuli has been reported by other groups [Geiger *et al.*, 2009; Li *et al.*, 2011]. Groups have also linked acetylation with microtubule stiffness [Felgner *et al.*, 1996; Hawkins *et al.*, 2013] and our findings support this paradigm. While acetylation remains to be directly connected to mechanical properties [Howes *et al.*, 2014], groups have proposed several mechanisms. Though acetylation does not seem to affect tubulin morphology or polymerization [Howes *et al.*, 2014; Soppina *et al.*, 2012], interactions between tubulin subunits may be affected by acetylation. Acetylation might also affect the recruitment of microtubule-associated proteins (MAPs). Their binding have been shown to stiffen microtubule nearly 4-fold [Felgner *et al.*, 1997]. To investigate this, future studies may use multiscale modeling to gain insights into the coupling of acetylation and mechanical properties. Previous studies have used coarse-grained simulations of tubulin dimers to determine tubulin hydrolysis leads to changes in tubulin conformation and deformation patterns [Mitra and Sept, 2008].

Although cilium stiffening can be attributed to acetylation, the changes in cilium orientation are likely explained by a different mechanism. During formation

of the cilium, the mother centriole seeds the cilium and later becomes the basal body with several anchoring appendages, including basal feet and striated rootlets [Kobayashi and Dynlacht, 2011]. These structures have been shown to determine the position of the mother centriole and are also thought to determine the orientation of the cilium [Farnum and Wilsman, 2011]. Varying the number and distribution of these anchoring structures are proposed to regulate cilium anchorage stiffness and orientation [Boisvieux-Ulrich and Sandoz, 1991; Kwon *et al.*, 2011]. The flow-induced changes in cilium protrusion may be attributed to these anchoring structures. Though the basal body's relation with the cellular microtubule network is not well understood, the cytoskeletal microtubules are likely more important to the nucleation and formation of the cilium. This network has been shown to increase in density at the basal body with flow [Espinha *et al.*, 2014]. Another mechanism that may regulate the mechanical properties of the cilium anchorage is increasing the microtubule attachments.

In summary, our data presents a new potential mechanism for the mechanosensory adaptation of the primary cilium. We show that cilium stiffness can be mechanically and chemically regulated. We also show acetylation is a process through which the cell can modulate its cilium stiffness, which also modulates the cellular mechanosensitivity. Our data also demonstrate that the cilium adapts quite rapidly. This short time scale is appealing when considering treatments for disorders with dysfunctional cellular mechanosensing. Future studies should elucidate acetylation's role in cellular mechanosensing, unlocking acetylation's potential as a therapy for these disorders.

Chapter 5

Analysis of primary cilia mechanosensation *in vivo*

Collaborators on this project are Yuan N. Young, Erik B. Malarkey, Bradley K. Yoder, and Christopher R. Jacobs.

5.1 Abstract

Several mathematical models have been developed to describe primary cilium deflection important in cellular mechanosensations and have reported the cilium's mechanical properties. However, until recently, cilium deflections have only been examined and described *in vitro*. Using a Cilia^{GFP} mouse allowing direct *in vivo* visualization of primary cilia, we present the first computational analysis of *in vivo* primary cilia deflection. Our stiffness findings are consistent with previously reported *in vitro* values. In contrast to *in vitro* bending behavior, *in vivo* cilia have a consistent rigid, non-bending base. Interestingly, we found cilium bending stiffness was strongly correlated with length. This novel combination of experimental and computational techniques provides a quantitative *in vivo* assessment of cilia behavior.

5.2 Introduction

Praetorius and Spring provided the first evidence of the cilium deflecting and connected this deflection to downstream biochemical signaling [Praetorius and Spring, 2001; Praetorius and Spring, 2003]. In addition to Praetorious and Spring's work in the kidney, other groups have now demonstrated primary cilia-mediated mechanosensation in the liver, bone, cartilage, vascular endothelium and embryonic node [Malone *et al.*, 2007; Masyuk *et al.*, 2006; McGrath *et al.*, 2003; Nauli *et al.*, 2008; Wann and Knight, 2012]. The primary cilium has additionally been implicated in diseases with impaired mechanosensation and disorders linked to cilium dysfunction are now classified as ciliopathies [Fliegauf *et al.*, 2007].

Surprisingly, although cilium mechanosensing has significant clinical implications, the mechanical behavior of the primary cilium remains poorly understood. Schwartz et al. first modeled the primary cilium as an elastic beam undergoing small deflections [Schwartz *et al.*, 1997]. Resnick and Hopfer similarly modeled the cilium exposed to rotational flow via an orbital shaker [Resnick and Hopfer, 2007]. Studies by Liu et al. and Rydhom et al. improved previous models by using more accurate descriptions of the load deflecting the cilium [Liu *et al.*, 2005; Rydholm *et al.*, 2010]. Our group has advanced these models by accounting for the initial position of the cilium and the contribution of the cilium's basal body [Downs *et al.*, 2012; Young *et al.*, 2012]. Although these studies have made promising advances, to date, all descriptions of cilia mechanical behavior have been reported from *in vitro* experiments.

In this study, we examined, for the first time, primary cilia deflections *in vivo*. We accomplished this by applying our modeling techniques to the recently generated Cilia^{GFP} mouse that allows direct visualization of primary cilia *in vivo* [O'Connor *et al.*, 2013]. Here, we report the first cilia stiffness measurements *in vivo* and confirmed *in vitro* measurements previously reported by our lab and others. We also revealed a surprising relationship between cilium bending stiffness and length. This novel combination of a mouse model and computational analysis provides a valuable technique to gain new insights into the primary cilium's mechanosensory function in physiologically relevant contexts.

5.3 Methods

5.3.1 *In vivo* imaging of renal cilia

This study was carried out in accordance with the guidelines of the University of Alabama at Birmingham Institutional Animal Care and Use Committee and the National Institutes of Health Guide for the Care and Use of Laboratory Animals. The mouse and *in vivo* imaging are previously described in detail [O'Connor *et al.*, 2013]. Briefly, under continuous anesthesia, the kidney of a Cilia^{GFP} mouse was exposed through a dorsal incision. The mouse positioned so that the kidney was on a coverslip over the objective (60× oil immersion, 1.49NA). Images were captured on a high-speed confocal microscope using fluorescein isothiocyanate filter (Chroma Technology, Rockingham, VT) with excitation by a 488 nm Argon laser (Melles Griot, Carlsbad, CA) (Figure 5.1). Using ImageJ, the coordinates of 26 primary cilia at rest and under flow in the kidney proximal tubule were determined and used for subsequent analysis.

5.3.2 Computational analysis

Each cilium was modeled as an elastic beam under hydrodynamic load and anchored by a torsional spring as previously described [Young *et al.*, 2012]. The cilium coordinates were normalized by the length of the cilium and parameterized as a function of the position along the cilium. The cilium position at rest was used to determine the internal stress within the cilium. The cilium position under flow was

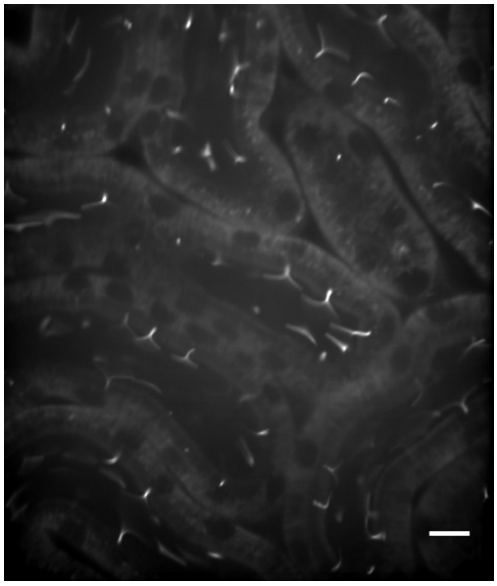

Figure 5.1: Fluorescent cilia in the kidney proximal tubule in an anesthetized mouse. Average fluorescence over 30 seconds illustrates the full bending behavior of each cilium. Strikingly, each cilium has a bending and non-bending portion. Scale bar indicates 10 μm.

used to determine the bending stiffness with a least squares fit. Glomerular filtration rate was used to approximate flow rate and the shear rate was determined assuming a Newtonian fluid within a pipe [Schnermann *et al.*, 2013]. A Pearson's r correlation analysis was performed between stiffness and length. Outliers were excluded by robust regression and outlier detection (Q = 1%; GraphPad, La Jolla, CA) [Motulsky and Brown, 2006]. All data are presented mean ± SEM.

5.4 Results

Cilia^{GFP} mice constitutively express a cilia marker, somatostatin receptor 3 fused to green fluorescent protein, that enabled cilia to be easily visualized. We first measured cilia length, 7.1 ± 0.3 μm (Figure 5.2A). Using a similar cilia-marker, *in vitro* studies have reported lengths of 5.2 ± 1.3 μm and 3.9 ± 0.8 μm in mouse inner medullary collecting duct cells [Downs *et al.*, 2012; Young *et al.*, 2012]. The difference in cilium length is likely attributed to the striking contrast between *in vivo* and *in vitro* conditions. Several factors influencing cilia length have been specifically identified, including mechanical stimuli and pharmacological agents [Miyoshi and Kasahara, 2011]. In contrast to *in vitro* studies, primary cilia in live mice exhibited a remarkably consistent non-bending region that extended 1.9 ± 0.1 μm from the base and accounted for 20 to 55% of the total cilium length (Figure 5.2B). While this may be attributed to cilium's molecular structure, including transition zone and ciliary pocket, the proximal tubule is abundant with microvilli [Guo *et al.*, 2000]. In the proximal tubule, the brush border microvilli are 2-3 μm projections and several orders of magnitude stiffer than primary cilia. The stiff microvilli surrounding each primary cilium may prevent the lower portion of each cilium from bending and thus, explain the rigid lower region of each cilium.

Here, we report the first stiffness measurements of primary cilia *in vivo*. We segmented each cilium into a bending and non-bending region and subsequently analyzed the bending region. We found bending stiffness of the ciliary axoneme to be 7.3 ± 0.1 × 10^{-23} Nm^2 and torsional stiffness anchoring the cilium to be 2.7 ± 0.7 × 10^{-8} Nm/rad (Figure 5.3). The *in vivo* bending stiffness was surprisingly

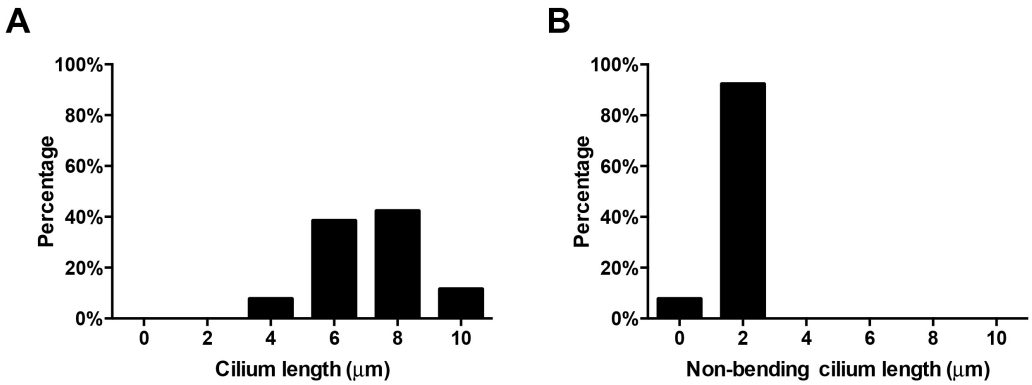

Figure 5.2: Distribution of primary cilium length in the kidney proximal tubules. The average total length of primary cilia was 7.1 ± 0.3 μm and the average length of the non-bending region was 1.9 ± 0.1 μm. We suspect this surprisingly consistent rigid region is due to microvilli.

consistent with the *in vitro* stiffness, 8.4×10^{-23} Nm^2, reported in our prior *in vitro* study [Young *et al.*, 2012]. We expected torque to be correlated to cilium length but did not find a significant correlation. Because a longer cilium is exposed to more fluid flow and must resist this larger load, we expected increased torque at the base of the cilium but found torque, rotational deflection, and torsional stiffness were consistent across lengths. Interestingly, we instead found a strong positive correlation between length and bending stiffness ($r = 0.55$, $p < 0.01$) (Figure 5.4). This is the first report that bending stiffness varies with length. We hypothesize that this may be to maintain consistent deflection and membrane strain across cilia in proximal tubules. Mechanosensitive channels found in the cilium, including Polycystin 1, Trpv4, and Piezo1, are activated by increases in membrane tension [Patel, 2014]. The increased membrane tension is believed to stretch or open these channels. In order to maintain consistent activation of these channels in a changing environment, the cilium may adapt its structural properties. For example longer cilia are exposed to more luminal fluid flow and may be stiffer to maintain a consistent degree of deflection when compared to shorter cilia in the same environment. With the recent development of techniques to measure membrane strain in live cells [Tabouillot *et al.*, 2011], we

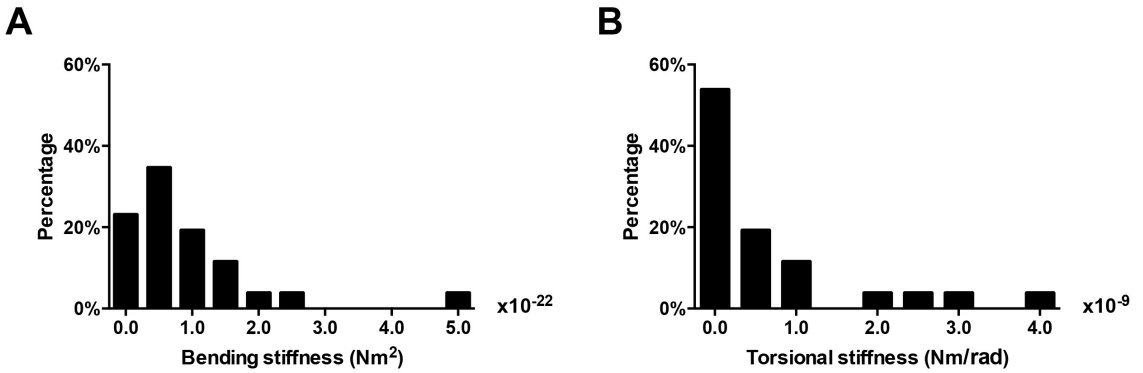

Figure 5.3: Distribution of primary cilia mechanical properties within the kidney proximal tubule. A) Bending stiffness of the ciliary shaft averaged 7.3 ± 0.1 × 10^{-23} Nm^2, excluding one outlier at 4.8 × 10^{-23} Nm^2. B) Torsional stiffness anchoring the cilium averaged 2.7 ± 0.7 × 10^{-8} Nm/rad, excluding four outliers between 1.8 and 4.1 × 10^{-23} Nm^2.

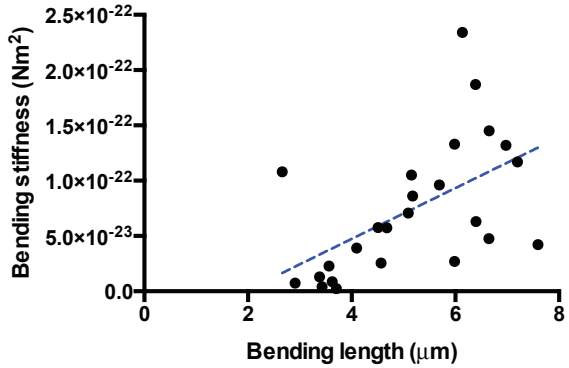

Figure 5.4: Correlation of primary cilia stiffness with length. Bending stiffness was strongly correlated with bending cilium length, r = 0.55 (n = 25, p < 0.01). This may be a result of cilia adapting to maintain consistent membrane strain with deflection. One outlier was removed using the robust regression and outlier removal method (Q = 1%)

will soon be able to determine how cilia deflection relates to ciliary membrane strain and if strain is consistent across a population of cilia.

5.5 Discussion

While the combination of our computational approach with this experimental data presents novel findings in primary cilia behavior, the study is not without its

limitations. We performed the analysis in two dimensions with epifluorescence images rather than three dimensions with z-stacks of confocal images as with prior *in vitro* studies. Although the loss of a dimension led to approximations in cilium position and flow, the agreement between the findings in this study with our previous *in vitro* studies suggests that the two-dimensional approach is sufficient. In addition, though we modeled flow as unidirectional and constant, there is suggestive evidence that renal tubular flow is not constant and can be pulsatile [O'Connor *et al.*, 2013]. With this more complex flow profile, the stiffness measurements reported are likely an over-approximation.

In this study, we combined experimental and computational techniques for a novel approach to describe primary cilia mechanical behavior and provide the first report of primary cilia stiffness *in vivo*. We found a strong agreement between these *in vivo* findings with prior *in vitro* measurements. This exciting investigational tool enables cilia mechanosensing to be quantified *in vivo* for the first time. Coupling this tool with disease models, we may quantitatively assess ciliary dysfunction in ciliopathies and in parallel, evaluate therapies that may restore this function.

Chapter 6

Conclusions

6.1 Summary

Mechanosensation is a ubiquitous process among living organisms and its dysfunction can lead to devastating diseases, including atherosclerosis, osteoporosis, and cancer. The primary cilium is an emerging mechanosensor already implicated in numerous biological contexts. The overarching objective of this dissertation was to characterize the mechanobiology of the cilium as a mechanosensor across biological scales. Collectively, our data suggest that the primary cilium is a complex signaling center that not only integrates mechanical signals and coordinates the biochemical responses, but is also able adapt in response to these signals. Specific contributions of this work are discussed below.

6.1.1 Primary cilia mechanosensation in bone by osteocytes *in vivo*

In chapter 2, we developed a conditional knockout mouse with primary cilia-deficient osteocytes and showed deleting primary cilia from osteocytes in mice leads to an impaired bone formation response to load. By deleting a gene with both ciliary and non-ciliary roles and targeting osteoblasts [Corbit *et al.*, 2008; Qiu *et al.*, 2012a; Temiyasathit *et al.*, 2012], prior studies had implicated osteocyte primary cilia but never directly examined osteocyte primary cilia *in vivo*. By targeting a cilia-specific gene, this study generated the first primary cilia-specific knockout in bone and by targeting osteocyte primary cilia specifically and examining them *in situ*, it presented the first evidence that deletion of a primary cilia gene led to loss of cilia in osteocytes. Prior studies had shown this loss occurred *in vitro* [Qiu *et al.*, 2012a; Temiyasathit *et al.*, 2012] but it remained unclear if a cilium present on an osteoblast remains as the osteoblast terminally differentiates into an osteocyte. Together, our data show *in vivo* that the primary cilium is an important sensing apparatus for the osteocyte, the principal mechanosensing cell in bone.

6.1.2 Lateral visualization of the cilium in assessing protein function

In chapter 3, we uncovered the need to standardize detection of ciliary proteins. We developed a classification system for proteins in the cilium and found for proteins present in the cilium and the rest of the cell, lateral imaging in addition to apical-basal

imaging is needed to distinguish proteins in the cilium from those in the rest of the cell. The majority of studies in our literature review only used apical-basal imaging and had erroneously excluded proteins from the cilium, suggesting that these proteins may need to be re-examined. Although this study was focused on immunocytochemistry, the conclusion to image cilia along multiple axes is an important consideration when imaging cilia in any context, including immunohistochemistry and *in vivo* imaging with the fluorescent cilia of the recently developed Cilia^{GFP} mouse [O'Connor *et al.*, 2013].

6.1.3 Primary cilia mechanosensation adapts and regulates cell signaling

In chapter 4, we use a combined experimental and computational approach to quantify the effect of mechanical and chemical stimuli on cilium deflection. Although prior studies had suggested the cilium's capacity to adapt [Besschetnova *et al.*, 2010; Downs *et al.*, 2012; McGlashan *et al.*, 2010], our study quantified these changes in the cilium's mechanical properties and identified a potential mechanism involved in the adaptation. We found that cilia stiffened in response to exposure to flow and with increased acetylation. We also found that increased acetylation decreases downstream cell signaling responses to flow. Together these data suggest that the cilium is a mechanosensor capable of structural adaptation and this adaptation mechanism involves acetylation. This is exciting for not only the cilia field but also the greater mechanosensing field, where sensory adaptation has remained controversial even in the most studied mechanosensors, ion channels.

6.1.4 Analysis of primary cilia mechanosensation *in vivo*

In chapter 5, we adapted our approach to analyze primary cilia deflection *in vivo*. Cilia^{GFP} mouse had recently been developed where primary cilia express a fluorescent marker [O'Connor *et al.*, 2013]. With fluorescence microscopy, we captured primary cilia deflection in the kidney proximal tubules of an anesthetized mouse. We found cilia had a consistent non-bending region that we attribute to the orders of magnitude stiffer microvilli. We calculated cilia bending stiffness and found our *in vivo* measurements were consistent with previous *in vitro* reports in the literature [Schwartz *et al.*, 1997; Downs *et al.*, 2012; Young *et al.*, 2012]. Even more compelling than this being the first analysis of *in vivo* primary cilia mechanics is the quantitative assessment of ciliary dysfunction in diseased mouse models now possible with this approach.

6.2 Future Directions

The studies presented in this dissertation have advanced our understanding of primary cilia as mechanosensors and their function across biological scales. While broadening our understanding of this organelle, our findings and the techniques developed have identified areas within this interplay of biology and mechanics to study further.

6.2.1 *In situ* analysis of primary cilia in bone

In chapter 2, we identified osteocyte primary cilia as a mechanosensing apparatus within bone. The pericellular space between the osteocyte body and lacunar wall is approximately 1 μm or less [Wassermann, 1965] while primary cilia from cultured osteocytes can be 2-9 μm in length [Malone *et al.*, 2007; Xiao *et al.*, 2006]. It remains unclear if the tight pericellular space allows for the primary cilia deflection observed *in vitro* [Downs *et al.*, 2012; Malone *et al.*, 2007; Praetorius and Spring, 2001; Schwartz *et al.*, 1997]. The goal of this future study would be to characterize primary cilia in bone. The increased penetration of the C3B9 antibody directed against acetylated α-tubulin [Poole *et al.*, 2001] and the Cilia^{GFP} mouse [O'Connor *et al.*, 2013] provide two different methods to visualize primary cilia *in situ*. An especially intriguing question is how are cilia distributed within bone. Previous reports of primary cilia incidence in bone have ranged from 4% [Baker *et al.*, 2003] to nearly 100% [Uzbekov *et al.*, 2012]. Leveraging our findings and methods on imaging cilia in chapter 3, this study may address the current controversy in bone primary cilia incidence. Another interesting question in bone is how are cilia

oriented within bone. Several studies in other tissues have suggested cilia orientation is influenced by load. For example, the orientation of cilia in load-bearing regions of cartilage was found to be consistent in contrast to non-load-bearing regions where the consistency is lost [Farnum and Wilsman, 2011]. Similarly, primary cilia are found to be highly oriented in tendon [Donnelly *et al.*, 2010]. Describing and characterizing the osteocyte primary cilium *in situ* will begin to answer how the osteocyte primary cilium senses load in the lacunar-canalicular system, a complex network of caverns and channels within bone.

In a second study, the goal would be to analyze osteocyte primary cilium deflection *in situ*. Our work in chapter 5 showed that primary cilium deflection in the kidney is easily visualized with the Cilia^{GFP} mouse. Preliminary work with bones harvested from this mouse reveal that it is possible to visualize the cilium but it is not without challenges. The osteocyte primary cilium is nearly an order of magnitude shorter than kidney primary cilium and is embedded in bone matrix. Recently, calcium signaling within osteocytes had been recorded *in situ* in bone [Ishihara *et al.*, 2012; Jing *et al.*, 2014], suggesting that although challenging, it may be possible to capture cilium deflection *in situ*. The recent development of these tools to visualize primary cilia *in situ* may finally answer the long-held questions about primary cilia in bone and further elucidate primary cilia-mediated mechanosensing in bone.

6.2.2 Primary cilia mechanosensation and adaptation in other cell types

In chapters 4 and 5, we analyzed renal primary cilia deflection *in vitro* and *in vivo*, respectively. Although deflection in response to flow has been observed *in vitro* with cilia from other cell types [Jensen *et al.*, 2004; Malone *et al.*, 2007], cilia deflection has not been quantitatively characterized outside of the kidney. A challenge with analyzing deflection is visualizing primary cilia. Directing fluorescent proteins to the cilium has proved to be problematic. In spite of many groups' efforts, only one cell line has been developed, the IMCD cells used in this work. However, it may now be possible to visualize primary cilia in other live cells using those isolated from the Cilia^{GFP} mouse. Thus, the goal of this study would be first, to quantitatively assess the deflection of cilia in other cell types and second, to determine if cilia of other cells also adapt. This can be done by isolating different cell types with fluorescing cilia from the Cilia^{GFP} mouse and applying similar techniques from our work in chapter 4. Our hypothesis is that cilia mechanical properties may vary from cell to cell but sensory adaptation is conserved.

6.2.3 Role of acetylation in primary cilia

Our data from chapter 4 strongly implicates acetylation in the stiffening of primary cilia. However, acetylation is poorly characterized and understood. The goal of this study would be to determine how acetylation modulates primary cilia stiffness. Acetylation does not affect the gross morphology but has been hypothesized to affect tubulin subunit interactions, limit access to the microtubule lumen, and

recruit microtubule-associated proteins [Felgner *et al.*, 1997; Howes *et al.*, 2014; Soppina *et al.*, 2012]. With the current technology, we are limited in experimentally exploring the relationship between acetylation and cilium stiffness. However, using modeling, it is possible to model acetylation and test the above hypothesis of acetylation affecting the subunit interactions. Coarse-graining can reduce the complexity of the model while still providing insights. For example, one study used coarse-graining of tubulin dimers and found that hydrolysis of tubulin led to a bend in the dimer [Gebremichael *et al.*, 2008]. Coarse-graining of the atoms within tubulin led to insights into the deformation patterns of each subunit. Using a similar approach and comparing to experiments of individual microtubules [Felgner *et al.*, 1997; Felgner *et al.*, 1996], a future study may determine if acetylation modulates cilia stiffness by altering tubulin subunit interactions.

6.2.4 Analysis of primary cilium membrane mechanics

Although the works in chapter 4 and 5 contribute to a greater understanding of primary cilia mechanosensing, many questions remain unanswered in the mechanics of primary cilia mechanosensing. For example, stretch-activated membrane channels found on the cilium are believed to play a critical role in cilia-mediated mechanotransduction [Gradilone *et al.*, 2007; Nauli *et al.*, 2003], suggesting cilium membrane tension is a critical component of mechanosensing. The goal of the future study would be to quantify cilia membrane tension under flow. This may be done using a recently developed technique that correlates the dynamics of fluorescent dyes introduced into the lipid bilayer with membrane tension [Muddana *et al.*, 2011]. While this has only been accomplished in the cell membrane, similar dyes have been

used to visualize membranes of motile cilia [Deiner *et al.*, 1993].We hypothesize that cilium membrane tension measurements will confirm suggestions from previous papers that membrane tension is highest at the base of the cilium [Rydholm *et al.*, 2010; Young *et al.*, 2012], where some stretch-activated channels have been found in higher concentrations [Fernandes *et al.*, 2008; Siroky *et al.*, 2006].

6.3 Concluding Remarks

The goal of this dissertation was to advance our understanding of the primary cilium as a mechanosensor by investigating the cilium's role in mechanosensing at the tissue level and the mechanics of the mechanosensing at the subcellular level. This was achieved through the experimental investigation and computational analysis where many of the tools and methods developed in the course of this work enable the pursuit of new areas in the study of primary cilia. This work has provided a clear demonstration of the cilium's role in the bone mechanosensing. Most importantly, this work has demonstrated the capacity of the cilium to adapt as a mechanosensor, quantified it and proposed a mechanism enabling the adaptation. This brings a new perspective to the primary cilia and the broader mechanosensing fields with potential implications to the treatment of the many diseases with impaired cellular mechanosensing.

Bibliography

[Anishkin and Sukharev, 2009] Andriy Anishkin and Sergei Sukharev. State-stabilizing interactions in bacterial mechanosensitive channel gating and adaptation. *The Journal of biological chemistry*, 284(29):19153–7, Jul 2009. 42

[Araki *et al.*, 1997] Kimi Araki, T Imaizumi, Keiji Okuyama, Y Oike, and K Yamamura. Efficiency of recombination by cre transient expression in embryonic stem cells: comparison of various promoters. *Journal of biochemistry*, 122(5):977–82, Nov 1997. 28

[Baker *et al.*, 2003] Sheila a Baker, Katie Freeman, Katherine Luby-Phelps, Gregory J Pazour, and Joseph C Besharse. Ift20 links kinesin ii with a mammalian intraflagellar transport complex that is conserved in motile flagella and sensory cilia. *The Journal of biological chemistry*, 278(36):34211–8, Sep 2003. 72

[Berbari *et al.*, 2008] Nicolas F Berbari, Andrew D Johnson, Jacqueline S Lewis, Candice C Askwith, and Kirk Mykytyn. Identification of ciliary localization sequences within the third intracellular loop of g protein-coupled receptors. *Molecular Biology of the Cell*, 19(April):1540–1547, 2008. 34, 38

[Besschetnova *et al.*, 2010] Tatiana Y Besschetnova, Elona Kolpakova-Hart, Yinghua Guan, Jing Zhou, Bjorn R Olsen, and Jagesh V Shah. Identification of signaling pathways regulating primary cilium length and flow-mediated adaptation. *Current biology: CB*, 20(2):182–7, Jan 2010. 6, 43, 49, 70

[Boisvieux-Ulrich and Sandoz, 1991] E Boisvieux-Ulrich and D Sandoz. Determination of ciliary polarity precedes differentiation in the epithelial cells of quail oviduct. *Biology of the cell / under the auspices of the European Cell Biology Organization*, 72(1-2):3–14, Jan 1991. 57

[Bonewald, 2011] Lynda F Bonewald. The amazing osteocyte. *Journal of bone and mineral research: the official journal of the American Society for Bone and Mineral Research*, 26(2):229–38, Feb 2011. 12, 27

[Bouxsein *et al.*, 2010] Mary L Bouxsein, Stephen K Boyd, Blaine a Christiansen, Robert E Guldberg, Karl J Jepsen, and Ralph Müller. Guidelines for assessment of bone

microstructure in rodents using micro-computed tomography. *Journal of bone and mineral research: the official journal of the American Society for Bone and Mineral Research*, 25(7):1468–86, Jul 2010. 17

[Burra *et al.*, 2010] Sirisha Burra, Daniel P Nicolella, W Loren Francis, Christopher J Freitas, Nicholas J Mueschke, Kristin Poole, and Jean X Jiang. Dendritic processes of osteocytes are mechanotransducers that induce the opening of hemichannels. *Proceedings of the National Academy of Sciences of the United States of America*, 107(31):13648–53, Aug 2010. 29

[Cardoso *et al.*, 2009] Luis Cardoso, Brad C Herman, Olivier Verborgt, Damien Laudier, Robert J Majeska, and Mitchell B Schaffler. Osteocyte apoptosis controls activation of intracortical resorption in response to bone fatigue. *Journal of bone and mineral research: the official journal of the American Society for Bone and Mineral Research*, 24(4):597–605, Apr 2009. 25

[Cheng *et al.*, 2001] B Cheng, S Zhao, J Luo, E Sprague, Lynda F Bonewald, and J X Jiang. Expression of functional gap junctions and regulation by fluid flow in osteocyte-like mlo-y4 cells. *Journal of bone and mineral research: the official journal of the American Society for Bone and Mineral Research*, 16(2):249–59, Feb 2001. 29

[Cherian *et al.*, 2005] Priscilla P Cherian, Arlene J Siller-jackson, Sumin Gu, Xin Wang, Lynda F Bonewald, Eugene Sprague, and Jean X Jiang. Mechanical strain opens connexin 43 hemichannels in osteocytes: A novel mechanism for the release of. *Molecular Biology of the Cell*, 16(July):3100–3106, 2005. 29

[Cho *et al.*, 2010] Andrew Cho, Shigeki Suzuki, Junko Hatakeyama, Naoto Haruyama, and Ashok B Kulkarni. A method for rapid demineralization of teeth and bones. *The open dentistry journal*, 4:223–9, Jan 2010. 18

[Choi *et al.*, 2011] Yun-Hee Choi, Akira Suzuki, Sachin Hajarnis, Zhendong Ma, Hannah C Chapin, Michael J Caplan, Marco Pontoglio, Stefan Somlo, and Peter Igarashi. Polycystin-2 and phosphodiesterase 4c are components of a ciliary a-kinase anchoring protein complex that is disrupted in cystic kidney diseases. *Proceedings of the National Academy of Sciences of the United States of America*, 108(26):10679–84, Jun 2011. 33, 38, 39

[Condon and Weinberger, 1991] C D Condon and N M Weinberger. Habituation produces frequency-specific plasticity of receptive fields in the auditory cortex. *Behavioral neuroscience*, 105(3):416–30, Jun 1991. 42

[Corbit *et al.*, 2005] Kevin C Corbit, Pia Aanstad, Veena Singla, Andrew R Norman, Didier Y R Stainier, and Jeremy F Reiter. Vertebrate smoothened functions at the primary cilium. *Nature*, 437(7061):1018–21, Oct 2005. 34, 38

[Corbit *et al.*, 2008] Kevin C Corbit, Amy E Shyer, William E Dowdle, Julie Gaulden, Veena Singla, Miao-Hsueh Chen, Pao-Tien Chuang, and Jeremy F Reiter. Kif3a constrains beta-catenin-dependent wnt signalling through dual ciliary and non-ciliary mechanisms. *Nature cell biology*, 10(1):70–6, Jan 2008. 13, 25, 69

[Dacquin *et al.*, 2002] Romain Dacquin, Michael Starbuck, Thorsten Schinke, and Gérard Karsenty. Mouse alpha1(i)-collagen promoter is the best known promoter to drive efficient cre recombinase expression in osteoblast. *Developmental dynamics: an official publication of the American Association of Anatomists*, 224(2):245–51, Jun 2002. 12

[Day *et al.*, 2005] Timothy F Day, Xizhi Guo, Lisa Garrett-Beal, and Yingzi Yang. Wnt/beta-catenin signaling in mesenchymal progenitors controls osteoblast and chondrocyte differentiation during vertebrate skeletogenesis. *Developmental cell*, 8(5):739–50, May 2005. 13, 29

[Deiner *et al.*, 1993] Michael Deiner, SL Tamm, and Signhild Tamm. Mechanical properties of ciliary axonemes and membranes as shown by paddle cilia. *Journal of cell science*, 1262:1251–1262, 1993. 76

[Delaine-Smith *et al.*, 2014] Robin M Delaine-Smith, Anuphan Sittichokechaiwut, and Gwendolen C Reilly. Primary cilia respond to fluid shear stress and mediate flow-induced calcium deposition in osteoblasts. *FASEB journal: official publication of the Federation of American Societies for Experimental Biology*, 28(1):430–9, Jan 2014. 11

[Dempster *et al.*, 2013] David W Dempster, Juliet E Compston, Marc K Drezner, Francis H Glorieux, John a Kanis, Hartmut Malluche, Pierre J Meunier, Susan M Ott, Robert R Recker, and a Michael Parfitt. Standardized nomenclature, symbols, and units for bone histomorphometry: a 2012 update of the report of the asbmr histomorphometry nomenclature committee. *Journal of bone and mineral research: the official journal of the American Society for Bone and Mineral Research*, 28(1):2–17, Jan 2013. 17

[Donnelly *et al.*, 2010] Eve Donnelly, Maria-Grazia Ascenzi, and Cornelia Farnum. Primary cilia are highly oriented with respect to collagen direction and long axis of extensor tendon. *Journal of orthopaedic researchâĂŕ: official publication of the Orthopaedic Research Society*, 28(1):77–82, Jan 2010. 73

[Downs *et al.*, 2012] Matthew E Downs, An M Nguyen, Florian A Herzog, David A Hoey, and Christopher R Jacobs. An experimental and computational analysis of primary cilia deflection under fluid flow. *Computer methods in biomechanics and biomedical engineering*, (April):37–41, Mar 2012. 6, 7, 44, 45, 49, 60, 64, 70, 71, 72

[Espinha *et al.*, 2014] Lina C. Espinha, David A. Hoey, Paulo R. Fernandes, Hélder C. Rodrigues, and Christopher R. Jacobs. Oscillatory fluid flow influences primary cilia and microtubule mechanics. *Cytoskeleton (Hoboken, N.J.)*, 71(7):435–45, Jul 2014. 45, 57

[Farnum and Wilsman, 2011] Cornelia E Farnum and Norman J Wilsman. Axonemal positioning and orientation in three-dimensional space for primary cilia: what is known, what is assumed, and what needs clarification. *Developmental dynamics: an official publication of the American Association of Anatomists*, 240(11):2405–31, Nov 2011. 57, 73

[Federman and Nichols, 1974] M Federman and G Nichols. Bone cell cilia: vestigial or functional organelles? *Calcified tissue research*, 17(1):81–5, Jan 1974. 2

[Felgner *et al.*, 1996] H Felgner, R Frank, and M Schliwa. Flexural rigidity of microtubules measured with the use of optical tweezers. *Journal of cell science*, 109 (Pt 2:509–16, Feb 1996. 50, 56, 75

[Felgner *et al.*, 1997] H Felgner, R Frank, J Biernat, E M Mandelkow, E Mandelkow, B Ludin, a Matus, and M Schliwa. Domains of neuronal microtubule-associated proteins and flexural rigidity of microtubules. *The Journal of cell biology*, 138(5):1067–75, Sep 1997. 56, 75

[Fernandes *et al.*, 2008] Jacqueline Fernandes, Ivan M Lorenzo, Yaniré N Andrade, Anna Garcia-Elias, Selma a Serra, José M Fernández-Fernández, and Miguel a Valverde. Ip3 sensitizes trpv4 channel to the mechano- and osmotransducing messenger 5'-6'-epoxyeicosatrienoic acid. *The Journal of cell biology*, 181(1):143–55, Apr 2008. 76

[Fliegauf *et al.*, 2007] Manfred Fliegauf, Thomas Benzing, and Heymut Omran. When cilia go bad: cilia defects and ciliopathies. *Nature reviews. Molecular cell biology*, 8(11):880–93, Nov 2007. 60

[Flores *et al.*, 2012] Daniel Flores, Yu Liu, Wen Liu, Lisa M Satlin, and Rajeev Rohatgi. Flow-induced prostaglandin e2 release regulates na and k transport in the collecting duct. *American journal of physiology. Renal physiology*, 303(5):F632–8, Sep 2012. 53

[Follit *et al.*, 2010] John a Follit, Lixia Li, Yvonne Vucica, and Gregory J Pazour. The cytoplasmic tail of fibrocystin contains a ciliary targeting sequence. *The Journal of cell biology*, 188(1):21–8, Jan 2010. 38

[Galbraith *et al.*, 2002] Catherine G Galbraith, Kenneth M Yamada, and Michael P Sheetz. The relationship between force and focal complex development. *The Journal of cell biology*, 159(4):695–705, Nov 2002. 43

[Galli *et al.*, 2010] C Galli, G Passeri, and G M Macaluso. Osteocytes and wnt: the mechanical control of bone formation. *Journal of dental research*, 89(4):331–43, Apr 2010. 13, 29

[Gebremichael *et al.*, 2008] Yeshitila Gebremichael, Jhih-Wei Chu, and Gregory a Voth. Intrinsic bending and structural rearrangement of tubulin dimer: molecular dynamics simulations and coarse-grained analysis. *Biophysical journal*, 95(5):2487–99, Sep 2008. 75

[Geiger *et al.*, 2009] R Christopher Geiger, Christopher D Kaufman, Ai P Lam, G R Scott Budinger, and David a Dean. Tubulin acetylation and histone deacetylase 6 activity in the lung under cyclic load. *American journal of respiratory cell and molecular biology*, 40(28):76–82, Jan 2009. 50, 56

[Geng *et al.*, 2006] Lin Geng, Dayne Okuhara, Zhiheng Yu, Xin Tian, Yiqiang Cai, Sekiya Shibazaki, and Stefan Somlo. Polycystin-2 traffics to cilia independently of polycystin-1 by using an n-terminal rvxp motif. *Journal of cell science*, 119(Pt 7):1383–95, Apr 2006. 34, 38

[Gradilone *et al.*, 2007] Sergio a Gradilone, Anatoliy I Masyuk, Patrick L Splinter, Jesus M Banales, Bing Q Huang, Pamela S Tietz, Tatyana V Masyuk, and Nicholas F Larusso. Cholangiocyte cilia express trpv4 and detect changes in luminal tonicity inducing bicarbonate secretion. *Proceedings of the National Academy of Sciences of the United States of America*, 104(48):19138–43, Nov 2007. 75

[Guo *et al.*, 2000] P Guo, a M Weinstein, and S Weinbaum. A hydrodynamic mechanosensory hypothesis for brush border microvilli. *American journal of physiology. Renal physiology*, 279(4):F698–712, Oct 2000. 64

[Haggarty *et al.*, 2003] Stephen J Haggarty, Kathryn M Koeller, Jason C Wong, Christina M Grozinger, and Stuart L Schreiber. Domain-selective small-molecule inhibitor of histone deacetylase 6 (hdac6)-mediated tubulin deacetylation. *Proceedings of the National Academy of Sciences of the United States of America*, 100(8):4389–94, Apr 2003. 50

[Harris, 2006] Raymond C Harris. Cox-2 and the kidney. *Journal of cardiovascular pharmacology*, 47 Suppl 1:S37–42, Jan 2006. 53

[Hawkins *et al.*, 2013] Taviare L Hawkins, David Sept, Binyam Mogessie, Anne Straube, and Jennifer L Ross. Mechanical properties of doubly stabilized microtubule filaments. *Biophysical journal*, 104(7):1517–28, Apr 2013. 50, 56

[Haycraft *et al.*, 2007] Courtney J Haycraft, Qihong Zhang, Buer Song, Walker S Jackson, Peter J Detloff, Rosa Serra, and Bradley K Yoder. Intraflagellar transport is essential for endochondral bone formation. *Development (Cambridge, England)*, 134(2):307–16, Jan 2007. 29

[Higginbotham *et al.*, 2012] Holden Higginbotham, Tae-Yeon Eom, Laura E Mariani, Amelia Bachleda, Joshua Hirt, Vladimir Gukassyan, Corey L Cusack, Cary Lai, Tamara Caspary, and E S Anton. Arl13b in primary cilia regulates the migration and placement of interneurons in the developing cerebral cortex. *Developmental cell*, 23(5):925–38, Nov 2012. 33

[Hirata *et al.*, 2014] Hiroaki Hirata, Hitoshi Tatsumi, Kimihide Hayakawa, and Masahiro Sokabe. Non-channel mechanosensors working at focal adhesion-stress fiber complex. *Pflugers Archive: European journal of physiology*, Jun 2014. 2, 43

[Hoey *et al.*, 2011] David a Hoey, Daniel J Kelly, and Christopher R Jacobs. A role for the primary cilium in paracrine signaling between mechanically stimulated osteocytes and mesenchymal stem cells. *Biochemical and biophysical research communications*, 412(1):182–7, Aug 2011. 11

[Hoey *et al.*, 2012] David a Hoey, Matthew E Downs, and Christopher R Jacobs. The mechanics of the primary cilium: an intricate structure with complex function. *Journal of biomechanics*, 45(1):17–26, Jan 2012.

[Hoffman *et al.*, 2011] Brenton D Hoffman, Carsten Grashoff, and Martin a Schwartz. Dynamic molecular processes mediate cellular mechanotransduction. *Nature*, 475(7356):316–23, Jul 2011. 2, 42

[Holmen *et al.*, 2005] Sheri L Holmen, Cassandra R Zylstra, Aditi Mukherjee, Robert E Sigler, Marie-Claude Faugere, Mary L Bouxsein, Lianfu Deng, Thomas L Clemens, and Bart O Williams. Essential role of beta-catenin in postnatal bone acquisition. *The Journal of biological chemistry*, 280(22):21162–8, Jun 2005. 13, 29

[Howes *et al.*, 2014] Stuart C Howes, Gregory M Alushin, Toshinobu Shida, Maxence V Nachury, and Eva Nogales. Effects of tubulin acetylation and tubulin acetyltransferase binding on microtubule structure. *Molecular biology of the cell*, 25(2):257–66, Jan 2014. 56, 75

[Humbert *et al.*, 2012] Melissa C Humbert, Katie Weihbrecht, Charles C Searby, Yalan Li, Robert M Pope, Val C Sheffield, and Seongjin Seo. Arl13b, pde6d, and cep164 form a functional network for inpp5e ciliary targeting. *Proceedings of the National Academy of Sciences of the United States of America*, 109(48):19691–6, 2012. 38

[Hurd *et al.*, 2011] Toby W Hurd, Shuling Fan, and Ben L Margolis. Localization of retinitis pigmentosa 2 to cilia is regulated by importin beta2. *Journal of cell science*, 124:718–726, 2011. 38

[Ishihara *et al.*, 2012] Yoshihito Ishihara, Yasuyo Sugawara, Hiroshi Kamioka, Noriaki Kawanabe, Hiroshi Kurosaka, Keiji Naruse, and Takashi Yamashiro. In situ imaging of the autonomous intracellular ca(2+) oscillations of osteoblasts and osteocytes in bone. *Bone*, 50(4):842–52, Apr 2012. 73

[Ishijima *et al.*, 2001] M Ishijima, S R Rittling, T Yamashita, K Tsuji, H Kurosawa, a Nifuji, D T Denhardt, and M Noda. Enhancement of osteoclastic bone resorption and suppression of osteoblastic bone formation in response to reduced mechanical stress do not occur in the absence of osteopontin. *The Journal of experimental medicine*, 193(3):399–404, Feb 2001. 29

[Jacobs *et al.*, 1998] C R Jacobs, C E Yellowley, B R Davis, Z Zhou, J M Cimbala, and H J Donahue. Differential effect of steady versus oscillating flow on bone cells. *Journal of biomechanics*, 31(11):969–76, Nov 1998. 45

[Janmey and McCulloch, 2007] Paul a Janmey and Christopher a McCulloch. Cell mechanics: integrating cell responses to mechanical stimuli. *Annual review of biomedical engineering*, 9:1–34, Jan 2007. 2

[Javaheri *et al.*, 2014] Behzad Javaheri, Amber Rath Stern, Nuria Lara, Mark Dallas, Hong Zhao, Ying Liu, Lynda F Bonewald, and Mark L Johnson. Deletion of a single Îš-catenin allele in osteocytes abolishes the bone anabolic response to loading. *Journal of bone and mineral research: the official journal of the American Society for Bone and Mineral Research*, 29(3):705–15, Mar 2014. 26

[Jenkins *et al.*, 2006] Paul M Jenkins, Toby W Hurd, Lian Zhang, Dyke P McEwen, R Lane Brown, Ben Margolis, Kristen J Verhey, and Jeffrey R Martens. Ciliary targeting of olfactory cng channels requires the cngb1b subunit and the kinesin-2 motor protein, kif17. *Current biology: CB*, 16(12):1211–6, Jun 2006. 38

[Jensen *et al.*, 2004] C G Jensen, C a Poole, S R McGlashan, M Marko, Z I Issa, K V Vujcich, and S S Bowser. Ultrastructural, tomographic and confocal imaging of the chondrocyte primary cilium in situ. *Cell biology international*, 28(2):101–10, Jan 2004. 74

[Jerome and Hoch, 2012] C Jerome and B Hoch. *Skeletal System*, chapter 5, pages 53 – 70. Academic Press, 2012. 29

[Jiang *et al.*, 2004] Di Jiang, Renny T Franceschi, Heidi Boules, and Guozhi Xiao. Parathyroid hormone induction of the osteocalcin gene. requirement for an osteoblast-specific element 1 sequence in the promoter and involvement of multiple-signaling pathways. *The Journal of biological chemistry*, 279(7):5329–37, Feb 2004. 12

[Jing *et al.*, 2014] Da Jing, Andrew D Baik, X Lucas Lu, Bin Zhou, Xiaohan Lai, Liyun Wang, Erping Luo, and X Edward Guo. In situ intracellular calcium oscillations in osteocytes in intact mouse long bones under dynamic mechanical loading. *FASEB journalâĂŕ: official publication of the Federation of American Societies for Experimental Biology*, 28(4):1582–92, Apr 2014. 73

[Kamel *et al.*, 2010] Mohamed a Kamel, Jason L Picconi, Nuria Lara-Castillo, and Mark L Johnson. Activation of Îš-catenin signaling in mlo-y4 osteocytic cells versus 2t3 osteoblastic cells by fluid flow shear stress and pge2: Implications for the study of mechanosensation in bone. *Bone*, 47(5):872–81, Nov 2010. 25

[Kobayashi and Dynlacht, 2011] Tetsuo Kobayashi and Brian D Dynlacht. Regulating the transition from centriole to basal body. *The Journal of cell biology*, 193(3):435–44, May 2011. 4, 27, 57

[Kodani *et al.*, 2013] Andrew Kodani, Maria Salomé Sirerol-Piquer, Allen Seol, Jose Manuel Garcia-Verdugo, and Jeremy F Reiter. Kif3a interacts with dynactin subunit p150 glued to organize centriole subdistal appendages. *The EMBO journal*, 32(4):597–607, Feb 2013. 29

[Kramer *et al.*, 2010] Ina Kramer, Christine Halleux, Hansjoerg Keller, Marco Pegurri, Jonathan H Gooi, Patricia Brander Weber, Jian Q Feng, Lynda F Bonewald, and Michaela Kneissel. Osteocyte wnt/beta-catenin signaling is required for normal bone homeostasis. *Molecular and cellular biology*, 30(12):3071–85, Jun 2010. 13, 29

[Kurahashi and Menini, 1997] T Kurahashi and A Menini. Mechanism of odorant adaptation in the olfactory receptor cell. *Nature*, 385(6618):725–9, Feb 1997. 42

[Kwon *et al.*, 2010] Ronald Y Kwon, Sara Temiyasathit, Padmaja Tummala, Clarence C Quah, and Christopher R Jacobs. Primary cilium-dependent mechanosensing is mediated by adenylyl cyclase 6 and cyclic amp in bone cells. *FASEB journal: official publication of*

the Federation of American Societies for Experimental Biology, 24(8):2859–68, Aug 2010. 11, 33, 35, 38, 43

[Kwon *et al.*, 2011] Ronald Y Kwon, David A Hoey, and Christopher R Jacobs. *Mechanobiology of Primary Cilia*. Springer, 2011. 57

[Larkins *et al.*, 2011] Christine E Larkins, Gladys D Gonzalez Aviles, Michael P East, Richard a Kahn, and Tamara Caspary. Arl13b regulates ciliogenesis and the dynamic localization of shh signaling proteins. *Molecular biology of the cell*, 22(23):4694–703, Dec 2011. 33, 38

[Lee *et al.*, 2014] Kristen L. Lee, David A. Hoey, Milos Spasic, Tong Tang, H Kirk Hammond, and Christopher R. Jacobs. Adenylyl cyclase 6 mediates loading-induced bone adaptation in vivo. *FASEB journal: official publication of the Federation of American Societies for Experimental Biology*, 28(3):1157–65, Mar 2014. 13, 16, 17, 18, 29

[Li *et al.*, 2011] Yuan Li, Julia S Chu, Kyle Kurpinski, Xian Li, Diana M Bautista, Li Yang, K-L Paul Sung, and Song Li. Biophysical regulation of histone acetylation in mesenchymal stem cells. *Biophysical journal*, 100(8):1902–9, Apr 2011. 50, 56

[Liang *et al.*, 2009] Chih-Chia Liang, Li-Ru You, Junn-Liang Chang, Ting-Fen Tsai, and Chun-Ming Chen. Transgenic mice exhibiting inducible and spontaneous cre activities driven by a bovine keratin 5 promoter that can be used for the conditional analysis of basal epithelial cells in multiple organs. *Journal of biomedical science*, 16:2, Jan 2009. 15

[Lin *et al.*, 2003] Fangming Lin, Thomas Hiesberger, Kimberly Cordes, Angus M Sinclair, Lawrence S B Goldstein, Stefan Somlo, and Peter Igarashi. Kidney-specific inactivation of the kif3a subunit of kinesin-ii inhibits renal ciliogenesis and produces polycystic kidney disease. *Proceedings of the National Academy of Sciences of the United States of America*, 100(9):5286–91, Apr 2003. 3

[Litzenberger *et al.*, 2009] Julie B. Litzenberger, Weishene Joyce Tang, Alesha B. Castillo, and Christopher R. Jacobs. Deletion of Îš1 integrins from cortical osteocytes reduces load-induced bone formation. *Cellular and Molecular Bioengineering*, 2(3):416–424, Jul 2009. 13, 16, 17, 26, 29

[Liu *et al.*, 2003] Wen Liu, Shiyun Xu, Craig Woda, Paul Kim, Sheldon Weinbaum, and Lisa M Satlin. Effect of flow and stretch on the [ca2+]i response of principal and intercalated cells in cortical collecting duct. *American journal of physiology. Renal physiology*, 285(5):F998–F1012, Nov 2003.

[Liu *et al.*, 2004] Fei Liu, Henning W Woitge, Alen Braut, Mark S Kronenberg, Alexander C Lichtler, Mina Mina, and Barbara E Kream. Expression and activity of osteoblast-targeted cre recombinase transgenes in murine skeletal tissues. *The International journal of developmental biology*, 48(7):645–53, Sep 2004. 12

[Liu *et al.*, 2005] Wen Liu, Noel S Murcia, Yi Duan, Sheldon Weinbaum, Bradley K Yoder, Erik Schwiebert, and Lisa M Satlin. Mechanoregulation of intracellular ca2+

concentration is attenuated in collecting duct of monocilium-impaired orpk mice. *American journal of physiology. Renal physiology*, 289(5):F978–88, Nov 2005. 60

[Liu *et al.*, 2007] Qin Liu, Glenn Tan, Natasha Levenkova, Tiansen Li, Edward N Pugh, John J Rux, David W Speicher, and Eric a Pierce. The proteome of the mouse photoreceptor sensory cilium complex. *Molecular and cellular proteomics: MCP*, 6(8):1299–317, Aug 2007. 6

[Loktev and Jackson, 2013] AlexanderV Loktev and PeterK Jackson. Neuropeptide y family receptors traffic via the bardet-biedl syndrome pathway to signal in neuronal primary cilia. *Cell Reports*, 5(5):1316–1329, 2013. 38

[Lu *et al.*, 2007] Y. Lu, Y. Xie, S. Zhang, V. Dusevich, L.F. Bonewald, and J.Q. Feng. Dmp1-targeted cre expression in odontoblasts and osteocytes. *Journal of Dental Research*, 86(4):320–325, Apr 2007. 15

[Lu, 2001] W. Lu. Comparison of pkd1-targeted mutants reveals that loss of polycystin-1 causes cystogenesis and bone defects. *Human Molecular Genetics*, 10(21):2385–2396, Oct 2001. 29

[Lucker *et al.*, 2010] Ben F Lucker, Mark S Miller, Slawomir a Dziedzic, Philip T Blackmarr, and Douglas G Cole. Direct interactions of intraflagellar transport complex b proteins ift88, ift52, and ift46. *The Journal of biological chemistry*, 285(28):21508–18, Jul 2010. 4

[Malone *et al.*, 2007] Amanda M D Malone, Charles T Anderson, Padmaja Tummala, Ronald Y Kwon, Tyler R Johnston, Tim Stearns, and Christopher R Jacobs. Primary cilia mediate mechanosensing in bone cells by a calcium-independent mechanism. *Proceedings of the National Academy of Sciences of the United States of America*, 104(33):13325–30, Aug 2007. 3, 11, 35, 60, 72, 74

[Marszalek *et al.*, 1999] J R Marszalek, P Ruiz-Lozano, E Roberts, K R Chien, and L S Goldstein. Situs inversus and embryonic ciliary morphogenesis defects in mouse mutants lacking the kif3a subunit of kinesin-ii. *Proceedings of the National Academy of Sciences of the United States of America*, 96(9):5043–8, Apr 1999. 12

[Masyuk *et al.*, 2006] Anatoliy I Masyuk, Tatyana V Masyuk, Patrick L Splinter, Bing Q Huang, Angela J Stroope, and Nicholas F LaRusso. Cholangiocyte cilia detect changes in luminal fluid flow and transmit them into intracellular ca2+ and camp signaling. *Gastroenterology*, 131(3):911–20, Sep 2006. 3, 60

[Masyuk *et al.*, 2013] Anatoliy I Masyuk, Bing Q Huang, Brynn N Radtke, Garbriella B Gajdos, Patrick L Splinter, Tatyana V Masyuk, Sergio a Gradilone, and Nicholas F Larusso. Ciliary subcellular localization of tgr5 determines the cholangiocyte functional response to bile acid signaling. *American journal of physiology. Gastrointestinal and liver physiology*, (507), Apr 2013. 38

[McGlashan *et al.*, 2010] Susan R McGlashan, Martin M Knight, Tina T Chowdhury, Purva Joshi, Cynthia G Jensen, Sarah Kennedy, and Charles a Poole. Mechanical loading

modulates chondrocyte primary cilia incidence and length. *Cell biology international*, 34(5):441–6, May 2010. 3, 70

[McGrath *et al.*, 2003] James McGrath, Stefan Somlo, Svetlana Makova, Xin Tian, and Martina Brueckner. Two populations of node monocilia initiate left-right asymmetry in the mouse. *Cell*, 114(1):61–73, Jul 2003. 3, 60

[Mitchell *et al.*, 2009] Kimberly a P Mitchell, Gabor Szabo, and Angela De S Otero. *Methods for the isolation of sensory and primary cilia–an overview.*, volume 94. Elsevier, first edit edition, Jan 2009. 7, 39

[Mitra and Sept, 2008] Arpita Mitra and David Sept. Taxol allosterically alters the dynamics of the tubulin dimer and increases the flexibility of microtubules. *Biophysical journal*, 95(7):3252–8, Oct 2008. 56

[Miyoshi and Kasahara, 2011] K Miyoshi and K Kasahara. Factors that influence primary cilium length. *Acta Med Okayama*, 65(5):279–285, 2011. 64

[Motulsky and Brown, 2006] Harvey J Motulsky and Ronald E Brown. Detecting outliers when fitting data with nonlinear regression - a new method based on robust nonlinear regression and the false discovery rate. *BMC bioinformatics*, 7:123, Jan 2006. 63

[Muddana *et al.*, 2011] Hari S Muddana, Ramachandra R Gullapalli, Evangelos Manias, and Peter J Butler. Atomistic simulation of lipid and dii dynamics in membrane bilayers under tension. *Physical chemistry chemical physicsâĂŤ: PCCP*, 13(4):1368–78, Jan 2011. 75

[Murcia *et al.*, 2000] N S Murcia, W G Richards, B K Yoder, M L Mucenski, J R Dunlap, and R P Woychik. The oak ridge polycystic kidney (orpk) disease gene is required for left-right axis determination. *Development (Cambridge, England)*, 127(11):2347–55, Jun 2000. 3, 29

[Naismith and Booth, 2012] James H Naismith and Ian R Booth. Bacterial mechanosensitive channels–mscs: evolution's solution to creating sensitivity in function. *Annual review of biophysics*, 41:157–77, Jan 2012. 42

[Nauli *et al.*, 2003] Surya M Nauli, Francis J Alenghat, Ying Luo, Eric Williams, Peter Vassilev, Xiaogang Li, Andrew E H Elia, Weining Lu, Edward M Brown, Stephen J Quinn, Donald E Ingber, and Jing Zhou. Polycystins 1 and 2 mediate mechanosensation in the primary cilium of kidney cells. *Nature genetics*, 33(2):129–37, Feb 2003. 33, 75

[Nauli *et al.*, 2008] Surya M Nauli, Yoshifumi Kawanabe, John J Kaminski, William J Pearce, Donald E Ingber, and Jing Zhou. Endothelial cilia are fluid shear sensors that regulate calcium signaling and nitric oxide production through polycystin-1. *Circulation*, 117(9):1161–71, Mar 2008. 3, 60

[Nguyen and Jacobs, 2013] An M Nguyen and Christopher R Jacobs. Emerging role of primary cilia as mechanosensors in osteocytes. *Bone*, 54(2):196–204, Jun 2013. 5

[O'Connor *et al.*, 2009] Amber K O'Connor, Robert a Kesterson, and Bradley K Yoder. *Generating conditional mutants to analyze ciliary functions: the use of Cre-lox technology to disrupt cilia in specific organs.*, volume 93. Elsevier, first edit edition, Jan 2009. 15

[O'Connor *et al.*, 2013] Amber K O'Connor, Erik B Malarkey, Nicolas F Berbari, Mandy J Croyle, Courtney J Haycraft, P Darwin Bell, Peter Hohenstein, Robert a Kesterson, and Bradley K Yoder. An inducible ciliagfp mouse model for in vivo visualization and analysis of cilia in live tissue. *Cilia*, 2(1):8, Jan 2013. 15, 61, 62, 67, 70, 71, 72

[Ou *et al.*, 2009] Young Ou, Yibing Ruan, Min Cheng, Joanna J Moser, Jerome B Rattner, and Frans a van der Hoorn. Adenylate cyclase regulates elongation of mammalian primary cilia. *Experimental cell research*, 315(16):2802–17, Oct 2009. 43

[Ou *et al.*, 2012] Young Ou, Ying Zhang, Min Cheng, Jerome B Rattner, Ina Dobrinski, and Frans a van der Hoorn. Targeting of crmp-2 to the primary cilium is modulated by gsk-3Îš. *PloS one*, 7(11):e48773, Jan 2012. 38

[Patel, 2014] Amanda Patel. The primary cilium calcium channels and their role in flow sensing. *Pflugers Archive: European journal of physiology*, Apr 2014. 65

[Pazour and Bloodgood, 2008] Gregory J Pazour and Robert a Bloodgood. *Targeting proteins to the ciliary membrane.*, volume 85. Elesvier Inc., 1 edition, Jan 2008.

[Phillips *et al.*, 2008] Jonathan a Phillips, Eduardo a C Almeida, Esther L Hill, J Ignacio Aguirre, Mercedes F Rivera, Inaam Nachbandi, Thomas J Wronski, Marjolein C H van der Meulen, and Ruth K Globus. Role for beta1 integrins in cortical osteocytes during acute musculoskeletal disuse. *Matrix biology: journal of the International Society for Matrix Biology*, 27(7):609–18, Sep 2008. 27, 29

[Poole *et al.*, 2001] C A Poole, Z J Zhang, and J M Ross. The differential distribution of acetylated and detyrosinated alpha-tubulin in the microtubular cytoskeleton and primary cilia of hyaline cartilage chondrocytes. *Journal of anatomy*, 199(Pt 4):393–405, Oct 2001. 18, 72

[Praetorius and Spring, 2001] H A Praetorius and K R Spring. Bending the mdck cell primary cilium increases intracellular calcium. *Journal of Membrane Biology*, 184(1):71–79, Nov 2001. 3, 60, 72

[Praetorius and Spring, 2003] H A Praetorius and K R Spring. Removal of the mdck cell primary cilium abolishes flow sensing. *The Journal of membrane biology*, 191(1):69–76, Jan 2003. 3, 60

[Praetorius and Spring, 2005] Helle a Praetorius and Kenneth R Spring. A physiological view of the primary cilium. *Annual review of physiology*, 67(Figure 1):515–29, Jan 2005. 4

[Pugh *et al.*, 1999] E N Pugh, S Nikonov, and T D Lamb. Molecular mechanisms of vertebrate photoreceptor light adaptation. *Current opinion in neurobiology*, 9(4):410–8, Aug 1999. 42

[Qian *et al.*, 2005] Feng Qian, Wen Wei, Gregory Germino, and Andres Oberhauser. The nanomechanics of polycystin-1 extracellular region. *The Journal of biological chemistry*, 280(49):40723–30, Dec 2005. 28

[Qiu *et al.*, 2012a] Ni Qiu, Zhousheng Xiao, Li Cao, Meagan M Buechel, Valentin David, Esra Roan, and L Darryl Quarles. Disruption of kif3a in osteoblasts results in defective bone formation and osteopenia. *Journal of cell science*, 125(Pt 8):1945–57, Apr 2012. 12, 13, 25, 26, 28, 69

[Qiu *et al.*, 2012b] Ni Qiu, Honghao Zhou, and Zhousheng Xiao. Downregulation of pkd1 by shrna results in defective osteogenic differentiation via camp/pka pathway in human mg-63 cells. *Journal of cellular biochemistry*, 113(3):967–76, Mar 2012. 11

[Quarmby and Parker, 2005] Lynne M Quarmby and Jeremy D K Parker. Cilia and the cell cycle? *The Journal of cell biology*, 169(5):707–10, Jun 2005. 6, 27

[Resnick and Hopfer, 2007] Andrew Resnick and Ulrich Hopfer. Force-response considerations in ciliary mechanosensation. *Biophysical journal*, 93(4):1380–90, Aug 2007. 60

[Rich and Clark, 2012] D. R. Rich and a. L. Clark. Chondrocyte primary cilia shorten in response to osmotic challenge and are sites for endocytosis. *Osteoarthritis and cartilage / OARS, Osteoarthritis Research Society*, 20(8):923–930, Apr 2012. 6

[Robling *et al.*, 2006] Alexander G Robling, Alesha B Castillo, and Charles H Turner. Biomechanical and molecular regulation of bone remodeling. *Annual review of biomedical engineering*, 8:455–98, Jan 2006. 2

[Rohatgi *et al.*, 2007] Rajat Rohatgi, Ljiljana Milenkovic, and Matthew P Scott. Patched1 regulates hedgehog signaling at the primary cilium. *Science (New York, N.Y.)*, 317(5836):372–6, Jul 2007. 33

[Rydholm *et al.*, 2010] Susanna Rydholm, Gordon Zwartz, Jacob M Kowalewski, Padideh Kamali-Zare, Thomas Frisk, and Hjalmar Brismar. Mechanical properties of primary cilia regulate the response to fluid flow. *American journal of physiology. Renal physiology*, (January 2010), Jan 2010. 43, 60, 76

[Sabsovich *et al.*, 2008] Ilya Sabsovich, J David Clark, Guochun Liao, Gary Peltz, Derek P Lindsey, Christopher R Jacobs, Wei Yao, Tian-Zhi Guo, and Wade S Kingery. Bone microstructure and its associated genetic variability in 12 inbred mouse strains: microct study and in silico genome scan. *Bone*, 42(2):439–51, Feb 2008. 17

[Santos and Reiter, 2014] Nicole Santos and Jeremy F Reiter. A central region of gli2 regulates its localization to the primary cilium and transcriptional activity. *Journal of cell science*, 127(Pt 7):1500–10, Apr 2014. 38

[Santos *et al.*, 2009] Ana Santos, Astrid D Bakker, Behrouz Zandieh-Doulabi, Cornelis M Semeins, and Jenneke Klein-Nulend. Pulsating fluid flow modulates gene expression of proteins involved in wnt signaling pathways in osteocytes. *Journal of orthopaedic*

research: official publication of the Orthopaedic Research Society, 27(10):1280–7, Oct 2009. 25

[Schnermann *et al.*, 2013] Jurgen Schnermann, Mona Oppermann, and Yuning Huang. Nephron filtration rate and proximal tubular fluid reabsorption in the akita mouse model of type i diabetes mellitus. *F1000Research*, 2:83, Jan 2013. 63

[Schwander *et al.*, 2010] Martin Schwander, Bechara Kachar, and Ulrich Müller. Review series: The cell biology of hearing. *The Journal of cell biology*, 190(1):9–20, Jul 2010. 2

[Schwartz *et al.*, 1997] EA Eric A Schwartz, ML L Leonard, Rena Bizios, and S S Bowser. Analysis and modeling of the primary cilium bending response to fluid shear. *The American journal of physiology*, 272(1 Pt 2):F132–8, Jan 1997. 4, 6, 50, 60, 71, 72

[Seo *et al.*, 2011] Seongjin Seo, Qihong Zhang, Kevin Bugge, David K. Breslow, Charles C. Searby, Maxence V. Nachury, and Val C. Sheffield. A novel protein lztfl1 regulates ciliary trafficking of the bbsome and smoothened. *PLoS Genetics*, 7(11), 2011. 38

[Sharma *et al.*, 2011] Neeraj Sharma, Zachary a Kosan, Jannese E Stallworth, Nicolas F Berbari, and Bradley K Yoder. Soluble levels of cytosolic tubulin regulate ciliary length control. *Molecular biology of the cell*, 22(6):806–16, Mar 2011.

[Shiba *et al.*, 2010] Dai Shiba, Danielle K Manning, Hisashi Koga, David R Beier, and Takahiko Yokoyama. Inv acts as a molecular anchor for nphp3 and nek8 in the proximal segment of primary cilia. *Cytoskeleton (Hoboken, N.J.)*, 67(2):112–9, Feb 2010. 33, 38

[Singla and Reiter, 2006] Veena Singla and Jeremy F Reiter. The primary cilium as the cell's antenna: signaling at a sensory organelle. *Science (New York, N.Y.)*, 313(5787):629–33, Aug 2006. 3

[Siroky *et al.*, 2006] Brian J Siroky, William B Ferguson, Amanda L Fuson, Yi Xie, Attila Fintha, Peter Komlosi, Bradley K Yoder, Erik M Schwiebert, Lisa M Guay-Woodford, and P Darwin Bell. Loss of primary cilia results in deregulated and unabated apical calcium entry in arpkd collecting duct cells. *American journal of physiology. Renal physiology*, 290(6):F1320–8, Jun 2006. 76

[Song *et al.*, 2007] Buer Song, Courtney J Haycraft, Hwa-seon Seo, Bradley K Yoder, and Rosa Serra. Development of the post-natal growth plate requires intraflagellar transport proteins. *Developmental biology*, 305(1):202–16, May 2007. 29

[Soppina *et al.*, 2012] Virupakshi Soppina, Jeffrey F Herbstman, Georgios Skiniotis, and Kristen J Verhey. Luminal localization of Îś-tubulin k40 acetylation by cryo-em analysis of fab-labeled microtubules. *PloS one*, 7(10):e48204, Jan 2012. 56, 75

[Stern *et al.*, 2012] Amber Rath Stern, Matthew M Stern, Mark E Van Dyke, Katharina Jähn, Matthew Prideaux, and Lynda F Bonewald. Isolation and culture of primary osteocytes from the long bones of skeletally mature and aged mice. *BioTechniques*, 52(6):361–73, Jun 2012. 27

[Su *et al.*, 2014] Xuefeng Su, Kaitlin Driscoll, Gang Yao, Anas Raed, Maoqing Wu, Philip L Beales, and Jing Zhou. Bardet-biedl syndrome proteins 1 and 3 regulate the ciliary trafficking of polycystic kidney disease 1 protein. *Human molecular genetics*, 2:1–11, Jun 2014. 33, 38

[Tabouillot *et al.*, 2011] Tristan Tabouillot, Hari S Muddana, and Peter J Butler. Endothelial cell membrane sensitivity to shear stress is lipid domain dependent. *Cellular and molecular bioengineering*, 4(2):169–181, Jun 2011. 65

[Tao *et al.*, 2009] Binli Tao, Su Bu, Zhihua Yang, Brian Siroky, John C Kappes, Andreas Kispert, and Lisa M Guay-Woodford. Cystin localizes to primary cilia via membrane microdomains and a targeting motif. *Journal of the American Society of Nephrology: JASN*, 20(12):2570–80, Dec 2009. 38

[Tarbell *et al.*, 2014] John M Tarbell, Scott I Simon, and Fitz-Roy E Curry. Mechanosensing at the vascular interface. *Annual review of biomedical engineering*, 16:505–32, Jul 2014. 2

[Tatsumi *et al.*, 2007] Sawako Tatsumi, Kiyoaki Ishii, Norio Amizuka, Minqi Li, Toshihiro Kobayashi, Kenji Kohno, Masako Ito, Sunao Takeshita, and Kyoji Ikeda. Targeted ablation of osteocytes induces osteoporosis with defective mechanotransduction. *Cell metabolism*, 5(6):464–75, Jun 2007. 7, 12, 25

[Temiyasathit *et al.*, 2012] Sara Temiyasathit, W Joyce Tang, Philipp Leucht, Charles T Anderson, Stefanie D Monica, Alesha B Castillo, Jill A Helms, Tim Stearns, and Christopher R Jacobs. Mechanosensing by the primary cilium: deletion of kif3a reduces bone formation due to loading. *PloS one*, 7(3):e33368, Jan 2012. 12, 13, 16, 17, 25, 26, 28, 69

[Trapp *et al.*, 2008] Melissa L. Trapp, Alevtina Galtseva, Danielle K. Manning, David R. Beier, Norman D. Rosenblum, and Lynne M. Quarmby. Defects in ciliary localization of nek8 is associated with cystogenesis. *Pediatric Nephrology*, 23:377–387, 2008. 38

[Tu *et al.*, 2012] Xiaolin Tu, Yumie Rhee, Keith W Condon, Nicoletta Bivi, Matthew R Allen, Denise Dwyer, Marina Stolina, Charles H Turner, Alexander G Robling, Lilian I Plotkin, and Teresita Bellido. Sost downregulation and local wnt signaling are required for the osteogenic response to mechanical loading. *Bone*, 50(1):209–17, Jan 2012. 13, 29

[Uzbekov *et al.*, 2012] R E Uzbekov, D B Maurel, P C Aveline, S Pallu, C L Benhamou, and G Y Rochefort. Centrosome fine ultrastructure of the osteocyte mechanosensitive primary cilium. *Microscopy and microanalysis: the official journal of Microscopy Society of America, Microbeam Analysis Society, Microscopical Society of Canada*, pages 1–12, Nov 2012. 39, 72

[Verborgt *et al.*, 2000] O Verborgt, G J Gibson, and M B Schaffler. Loss of osteocyte integrity in association with microdamage and bone remodeling after fatigue in vivo. *Journal of bone and mineral research: the official journal of the American Society for Bone and Mineral Research*, 15(1):60–7, Jan 2000. 25

[Wann and Knight, 2012] a K T Wann and M M Knight. Primary cilia elongation in response to interleukin-1 mediates the inflammatory response. *Cellular and molecular life sciences: CMLS*, 69(17):2967–77, Sep 2012. 60

[Ward *et al.*, 2011] H. H. Ward, U. Brown-Glaberman, J. Wang, Y. Morita, S. L. Alper, E. J. Bedrick, V. H. Gattone, D. Deretic, and a. Wandinger-Ness. A conserved signal and gtpase complex are required for the ciliary transport of polycystin-1. *Molecular Biology of the Cell*, 22:3289–3305, 2011. 38

[Wassermann, 1965] F. Wassermann. Fine structure of the osteocyte capsule and of the wall of the lacunae in bone. *Cell and Tissue Research*, 67(5):636–652, 1965. 72

[Waters and Beales, 2011] Aoife M Waters and Philip L Beales. Ciliopathies: an expanding disease spectrum. *Pediatric nephrology (Berlin, Germany)*, 26(7):1039–56, Jul 2011. 3

[Wetzel *et al.*, 2001] Christian H. Wetzel, Marc Spehr, and Hanns Hatt. Phosphorylation of voltage-gated ion channels in rat olfactory receptor neurons. *European Journal of Neuroscience*, 14(7):1056–1064, Oct 2001.

[Wheatley and Bowser, 2000] Denys N. Wheatley and Samuel S. Bowser. Length control of primary cilia: analysis of monociliate and multiciliate ptk1 cells. *Biology of the cell / under the auspices of the European Cell Biology Organization*, 92(8-9):573–82, Dec 2000. 39

[Wheatley *et al.*, 1996] D N Wheatley, a M Wang, and G E Strugnell. Expression of primary cilia in mammalian cells. *Cell biology international*, 20(1):73–81, Jan 1996. 6, 27

[Wheatley, 1995] D N Wheatley. Primary cilia in normal and pathological tissues. *Pathobiology: journal of immunopathology, molecular and cellular biology*, 63(4):222–38, Jan 1995.

[Whitfield, 2003] James F Whitfield. Primary cilium–is it an osteocyte's strain-sensing flowmeter? *Journal of cellular biochemistry*, 89(2):233–7, May 2003. 11

[Wu *et al.*, 2012] V. M. Wu, S. C. Chen, M. R. Arkin, and J. F. Reiter. Small molecule inhibitors of smoothened ciliary localization and ciliogenesis. *Proceedings of the National Academy of Sciences*, 109(34):13644–13649, 2012. 38

[Xiao *et al.*, 2006] Zhousheng Xiao, Shiqin Zhang, Josh Mahlios, Gan Zhou, Brenda S Magenheimer, Dayong Guo, Sarah L Dallas, Robin Maser, James P Calvet, Lynda F Bonewald, and Leigh Darryl Quarles. Cilia-like structures and polycystin-1 in osteoblasts/osteocytes and associated abnormalities in skeletogenesis and runx2 expression. *The Journal of biological chemistry*, 281(41):30884–95, Oct 2006. 3, 11, 29, 72

[Xiao *et al.*, 2010] Zhousheng Xiao, Shiqin Zhang, Li Cao, Ni Qiu, Valentin David, and L Darryl Quarles. Conditional disruption of pkd1 in osteoblasts results in osteopenia due to direct impairment of bone formation. *The Journal of biological chemistry*, 285(2):1177–87, Jan 2010. 28, 29

[Xiao *et al.*, 2011] Zhousheng Xiao, Mark Dallas, Ni Qiu, Daniel Nicolella, Li Cao, Mark Johnson, Lynda F Bonewald, and L Darryl Quarles. Conditional deletion of pkd1 in osteocytes disrupts skeletal mechanosensing in mice. *FASEB journal: official publication of the Federation of American Societies for Experimental Biology*, 25(7):2418–32, Jul 2011. 14, 28, 29

[Xu *et al.*, 2007] Chang Xu, Sandro Rossetti, Lianwei Jiang, Peter C Harris, Ursa Brown-Glaberman, Angela Wandinger-Ness, Robert Bacallao, and Seth L Alper. Human adpkd primary cyst epithelial cells with a novel, single codon deletion in the pkd1 gene exhibit defective ciliary polycystin localization and loss of flow-induced ca2+ signaling. *American journal of physiology. Renal physiology*, 292(3):F930–45, Mar 2007. 38

[Yang *et al.*, 2005] Wuchen Yang, Yongbo Lu, Ivo Kalajzic, Dayong Guo, Marie a Harris, Jelica Gluhak-Heinrich, Shiva Kotha, Lynda F Bonewald, Jian Q Feng, David W Rowe, Charles H Turner, Alexander G Robling, and Stephen E Harris. Dentin matrix protein 1 gene cis-regulation: use in osteocytes to characterize local responses to mechanical loading in vitro and in vivo. *The Journal of biological chemistry*, 280(21):20680–90, May 2005. 13

[Yoder, 2002] B. K. Yoder. The polycystic kidney disease proteins, polycystin-1, polycystin-2, polaris, and cystin, are co-localized in renal cilia. *Journal of the American Society of Nephrology*, 13(10):2508–2516, Oct 2002. 3, 29, 38

[You *et al.*, 2001] L You, S C Cowin, M B Schaffler, and S Weinbaum. A model for strain amplification in the actin cytoskeleton of osteocytes due to fluid drag on pericellular matrix. *Journal of biomechanics*, 34(11):1375–86, Nov 2001. 29

[Young *et al.*, 2012] Yuan N Young, Matthew E Downs, and Christopher R Jacobs. Dynamics of the primary cilium in shear flow. *Biophysical journal*, 103(4):629–39, Aug 2012. 7, 44, 45, 46, 49, 60, 62, 64, 65, 71, 76

[Young *et al.*, 2014] Yuan N Young, Lina C Espinha, An M Nguyen, and Christopher R Jacobs. *Primary Cilia: Multi-Scale Structures that integrate Biomechanics and Mechanobiology*. Springer, 2014.

[Zhang *et al.*, 2003] Qihong Zhang, Noel S Murcia, Laura R Chittenden, William G Richards, Edward J Michaud, Richard P Woychik, and Bradley K Yoder. Loss of the tg737 protein results in skeletal patterning defects. *Developmental dynamics: an official publication of the American Association of Anatomists*, 227(1):78–90, May 2003. 29